

# Generating cosmological perturbations at Horndeski bounce

Y. Ageeva<sup>a,b,c,1</sup>, P. Petrov<sup>a,2</sup>, V. Rubakov<sup>a,b,3</sup>

<sup>a</sup> *Institute for Nuclear Research of the Russian Academy of Sciences,  
60th October Anniversary Prospect, 7a, 117312 Moscow, Russia*

<sup>b</sup> *Department of Particle Physics and Cosmology,  
Physics Faculty, M.V. Lomonosov Moscow State University,  
Leninskie Gory 1-2, 119991 Moscow, Russia*

<sup>c</sup> *Institute for Theoretical and Mathematical Physics,  
M.V. Lomonosov Moscow State University,  
Leninskie Gory 1, 119991 Moscow, Russia*

## Abstract

We construct a concrete model of Horndeski bounce with strong gravity in the past. Within this model we show that the correct spectra of cosmological perturbations may be generated at early contracting epoch, with mild fine-tuning ensuring that the scalar spectral tilt  $n_S$  and tensor-to-scalar ratio  $r$  are consistent with observations. The smallness of  $r$  is governed by the smallness of the scalar sound speed. Arbitrarily small values of  $r$  are forbidden in our setup because of the strong coupling in the past. Nevertheless, we show that it is possible to generate perturbations in a controllable way, i.e. in the regime where the background evolution and perturbations are legitimately described within classical field theory and weakly coupled quantum theory.

## 1 Introduction

Bouncing Universe is an interesting alternative to inflation; for reviews and general discussion see, e.g., Refs. [1, 2, 3, 4, 5, 6]. Its realization within classical field theory requires the violation of the null convergence condition (null energy condition in General Relativity).

---

<sup>1</sup>**email:** ageeva@inr.ac.ru

<sup>2</sup>**email:** petrov@inr.ac.ru

<sup>3</sup>**email:** rubakov@inr.ac.ru

One set of models where this property may occur without obvious pathologies is the class of Horndeski theories [7]; explicit examples of healthy bouncing stages are numerous in these theories [8, 9, 10, 11, 12, 13, 14, 15], for reviews see, e.g., Refs. [16, 17]. Within Horndeski theories, extending bouncing cosmology to the whole time interval  $-\infty < t < +\infty$  is not straightforward, however. Namely, perturbations about bouncing spatially flat FLRW backgrounds  $ds^2 = -dt^2 + a^2(t)\delta_{ij}dx^i dx^j$  have either gradient or ghost instabilities, or both, provided that the following two integrals diverge:

$$\int_{-\infty}^t a(t)(\mathcal{F}_T + \mathcal{F}_S)dt = \infty , \quad (1a)$$

$$\int_t^{+\infty} a(t)(\mathcal{F}_T + \mathcal{F}_S)dt = \infty , \quad (1b)$$

where  $\mathcal{F}_T$  and  $\mathcal{F}_S$  are time-dependent coefficients in the quadratic actions for tensor (transverse traceless  $h_{ij}$ ) and scalar ( $\zeta$ ) perturbations,

$$\mathcal{S}_{hh} = \int dt d^3x \frac{a^3}{8} \left[ \mathcal{G}_T \dot{h}_{ij}^2 - \frac{\mathcal{F}_T}{a^2} h_{ij,k} h_{ij,k} \right] , \quad (2a)$$

$$\mathcal{S}_{\zeta\zeta} = \int dt d^3x a^3 \left[ \mathcal{G}_S \dot{\zeta}^2 - \frac{\mathcal{F}_S}{a^2} \zeta_{,i} \zeta_{,i} \right] . \quad (2b)$$

This property, known as the no-go theorem [18, 19, 20, 21], rules out the simplest bouncing Horndeski setups where  $a(t)$  tends to infinity while  $\mathcal{F}_T$  and  $\mathcal{F}_S$  stay positive and finite as  $t \rightarrow \pm\infty$ .

One way [22, 23, 24, 25, 26, 27] of getting around this theorem is to employ beyond Horndeski theories [28, 29] Degenerate Higher-Order Scalar-Tensor (DHOST) generalizations [30]. These, however, have their own problems, since adding conventional matter fields often results in superluminality [31]. Without employing these generalizations, i.e., staying within the Horndeski class, there is still a possibility to allow the coefficients  $\mathcal{G}_T$ ,  $\mathcal{F}_T$ ,  $\mathcal{G}_S$  and  $\mathcal{F}_S$  to tend to zero as  $t \rightarrow -\infty$  in such a way that the integral in the left hand side of (1a) converges in the lower limit [19]. At first sight this is dangerous from the viewpoint of strong coupling: the coefficients  $\mathcal{G}_T$ ,  $\mathcal{F}_T$ ,  $\mathcal{G}_S$  and  $\mathcal{F}_S$  are analogs of the Planck mass squared, so their early-time behavior  $\mathcal{G}_T, \mathcal{F}_T, \mathcal{G}_S, \mathcal{F}_S \rightarrow 0$  as  $t \rightarrow -\infty$  implies that the gravitational interaction is strong in remote past; note that we always work in the Jordan frame and that  $a(t)$  grows backwards in time at early times. Nevertheless, depending on the model, the cosmological evolution may, in fact, be legitimately described within classical field theory at all times, since even at early times the classical energy scale (which is  $|t|^{-1}$  for power-law bounce) may be lower than the quantum strong coupling scale [32, 33, 34, 35]. It is worth emphasizing that this idea of healthy bounce with “strong gravity in the past” (meaning that  $\mathcal{G}_T, \mathcal{F}_T, \mathcal{G}_S, \mathcal{F}_S \rightarrow 0$  as  $t \rightarrow -\infty$ ) has been re-invented, albeit not quite explicitly, in

Refs. [36, 37] from a different prospective: bounce in the Jordan frame is obtained there via conformal transformation from an inflationary setup in the Einstein frame. Unlike in Refs. [36, 37], we work directly in the Jordan frame.

It is relatively straightforward to construct Horndeski models which admit bouncing solutions with power-law asymptotics at early times [19, 35],

$$a(t) \propto (-t)^\chi, \quad \mathcal{G}_T, \mathcal{F}_T, \mathcal{G}_S, \mathcal{F}_S \propto \frac{1}{(-t)^{2\mu}}, \quad t \rightarrow -\infty, \quad (3)$$

with time-independent parameters  $1 > \chi > 0$ ,  $2\mu > \chi + 1$ . The latter property guarantees that the inequality (1a) does not hold, which is a pre-requisite for healthy bounce. In this paper we concentrate on this simple case and consider the generation of cosmological perturbations at early contraction stage. In terms of conformal time  $\eta \propto -(-t)^{1-\chi}$ , the quadratic action (2a) for tensor perturbations coincides with that in General Relativity with the background scale factor

$$a_E(\eta) = a(\eta)\mathcal{G}_T^{1/2}(\eta) \propto \frac{1}{(-\eta)^{\frac{\mu-\chi}{1-\chi}}}. \quad (4)$$

In fact, this is precisely the scale factor in the Einstein frame in our class of models. Now, for  $\mu < 1$  the Einstein frame cosmic time  $t_E = \int a_E(\eta)d\eta = -(-\eta)^{\frac{1-\mu}{1-\chi}}$  runs from  $t_E = -\infty$ , and the effective scale factor increases as  $a_E = (-t_E)^{-b}$  where  $b = \frac{\mu-\chi}{1-\mu} > 1$  [33]. Such a geometry is singular as  $t_E \rightarrow -\infty$ : it is past geodesically incomplete and cannot be completed<sup>1</sup>. On the other hand, for  $\mu > 1$  one immediately recognizes effective power-law inflation with

$$a_E(t) \propto t_E^{\frac{\mu-\chi}{1-\mu}}, \quad (5)$$

where  $t_E = (-\eta)^{-\frac{\mu-1}{1-\chi}}$  runs from  $t_E = 0$ . In the Einstein frame, this is a version of  $G$ -inflation [38]. In either case, for  $\mu \approx 1$  the Einstein frame expansion is nearly exponential, so the power spectrum of generated tensor perturbations is nearly flat; similar observation applies to scalar perturbations as well. This implies that Horndeski bounce with “strong gravity in the past” may be capable of generating realistic cosmological perturbations; we again emphasize the similarity with Refs. [36, 37, 38] (where approximate flatness of the spectra is built in by construction).

In this paper we consider the models from the class of Refs. [19, 35], as described below. The issues we would like to understand are: (i) what governs spectral tilts and the overall amplitudes of scalar and tensor perturbations; (ii) is it possible to obtain small tensor-to-scalar ratio  $r = \mathcal{P}_h/\mathcal{P}_\zeta$  and, if so, what sort of tuning is required for that; (iii) is it possible to generate perturbations in a controllable way, i.e., in the regime where the background evolution

---

<sup>1</sup>This property is not pathological in our case, since by assumption particles with time-independent mass feel the Jordan frame geometry rather than the Einstein frame one.

and perturbations are legitimately described within classical field theory and weakly coupled quantum theory, respectively — and if so, does this constrain the values of observables.

We emphasize that we design and study our models in the Jordan frame where they have fairly simple structure. We could equivalently work in the Einstein frame, but then the analysis would be more cumbersome. We comment on the Einstein frame counterparts of our findings where appropriate.

An alert reader would anticipate that the spectral tilts (both scalar and tensor) are to large extent determined by the value of  $\mu$  in (3); in particular, red tilts occur at  $\mu > 1$ . This is indeed the case, see Sec. 2.3. In this paper we mostly stick to the  $\Lambda$ CDM value of the scalar spectral index [39],

$$n_S = 0.9649 \pm 0.0042 . \quad (6)$$

We comment, however, that the possible presence of early dark energy makes the scale invariant Harrison–Zeldovich spectrum with  $n_S = 1$  consistent with observations [40, 41]. Hence, we also briefly consider a bounce model with the flat power spectrum.

This paper is organized as follows. We introduce our class of Horndeski models and discuss early contracting stage of bouncing universe in Secs. 2.1, 2.2. We derive the properties of linearized scalar and tensor perturbations generated at that stage in Sec. 2.3, while in Sec. 2.4 we point out the relation between the flatness of the spectra and approximate dilatation invariance of the models. Sections 2.5 and 2.6 are central in our relatively general discussion in Sec. 2: we observe that there is tension between the small value of  $r$  (and to lesser extent the red scalar spectral tilt), on the one hand, and the requirement of the absence of strong coupling, on the other. We consider this issue at qualitative level in Sec. 2.5 and proceed to quantitative analysis in Sec. 2.6. We illustrate this tension in Sec. 3, where we derive lower bounds on  $r$  in very concrete models, first with the  $\Lambda$ CDM scalar tilt (6), and then with  $n_S = 1$ . We conclude in Sec. 4. Appendices A, B, and C contain details of more technical character.

## 2 Horndeski models with power-law contraction

### 2.1 Preliminaries

We consider a subclass of Horndeski theories whose action has the form (in the Jordan frame)

$$\mathcal{S} = \int d^4x \sqrt{-g} \{ G_2(\phi, X) - G_3(\phi, X) \square\phi + G_4(\phi, X) R + G_{4X} [(\square\phi)^2 - (\nabla_\mu \nabla_\nu \phi)^2] \} , \quad (7)$$

$$X = -\frac{1}{2} g^{\mu\nu} \partial_\mu \phi \partial_\nu \phi ,$$

where  $\square\phi = g^{\mu\nu} \nabla_\mu \nabla_\nu \phi$  and  $(\nabla_\mu \nabla_\nu \phi)^2 = \nabla_\mu \nabla_\nu \phi \nabla^\mu \nabla^\nu \phi$ ,  $R$  is the Ricci scalar. The metric signature is  $(-, +, +, +)$ . Unlike the general Horndeski theory, the Lagrangian (7) involves

three arbitrary functions  $G_{2,3,4}$  rather than four. It is convenient to work in the ADM formalism [16]. To this end, the metric is written as

$$ds^2 = -N^2 d\hat{t}^2 + \gamma_{ij} (dx^i + N^i d\hat{t}) (dx^j + N^j d\hat{t}) ,$$

where  $\gamma_{ij}$  is three-dimensional metric,  $N$  is the lapse function and  $N_i = \gamma_{ij} N^j$  is the shift vector. We denote the general time variable by  $\hat{t}$  and reserve the notation  $t$  for cosmic time. By choosing the unitary gauge (in which  $\phi$  depends on  $\hat{t}$  only and has prescribed form  $\phi = \phi(\hat{t})$ ), one rewrites the action as follows,

$$\mathcal{S} = \int d^4x \sqrt{-g} [A_2(\hat{t}, N) + A_3(\hat{t}, N)K + A_4(\hat{t}, N)(K^2 - K_{ij}^2) + B_4(\hat{t}, N)R^{(3)}] , \quad (8)$$

where

$$A_4(\hat{t}, N) = -B_4(\hat{t}, N) - N \frac{\partial B_4(\hat{t}, N)}{\partial N} ,$$

${}^{(3)}R_{ij}$  is the Ricci tensor made of  $\gamma_{ij}$ ,  $\sqrt{-g} = N\sqrt{\gamma}$ ,  $K = \gamma^{ij} K_{ij}$ ,  ${}^{(3)}R = \gamma^{ij} {}^{(3)}R_{ij}$  and

$$K_{ij} \equiv \frac{1}{2N} \left( \frac{d\gamma_{ij}}{d\hat{t}} - {}^{(3)}\nabla_i N_j - {}^{(3)}\nabla_j N_i \right) ,$$

is extrinsic curvature of hypersurfaces  $\hat{t} = \text{const}$ . The relationship between the Lagrangian functions in the covariant and ADM formalisms is given by [29, 42, 43]

$$G_2 = A_2 - 2XF_\phi, \quad G_3 = -2XF_X - F, \quad G_4 = B_4 , \quad (9)$$

where  $N$  and  $X$  are related by

$$N^{-1} d\phi/d\hat{t} = \sqrt{2X} , \quad (10)$$

and

$$F_X = -\frac{A_3}{(2X)^{3/2}} - \frac{B_4\phi}{X} . \quad (11)$$

We note in passing a subtlety here. Equation (11) defines  $F(\phi, X)$  up to additive term  $D(\phi)$ . This term modifies the Lagrangian functions,

$$G_2 \rightarrow G_2 - 2XD_\phi , \quad G_3 \rightarrow G_3 - D .$$

However, the additional contribution to the action (7) vanishes upon integration by parts,

$$\int d^4x \sqrt{-g} (-2XD_\phi + D\Box\phi) = \int d^4x \sqrt{-g} \nabla_\mu (D\nabla^\mu\phi) = 0 . \quad (12)$$

Therefore, this freedom is, in fact, irrelevant.

To describe FLRW background and perturbations about it, one writes

$$N = N_0(\hat{t})(1 + \alpha) , \quad (13a)$$

$$N_i = \partial_i \beta + N_i^T , \quad (13b)$$

$$\gamma_{ij} = a^2(\hat{t}) \left( e^{2\zeta} (e^h)_{ij} + \partial_i \partial_j Y + \partial_i W_j^T + \partial_j W_i^T \right) , \quad (13c)$$

where  $a(\hat{t})$  and  $N_0(\hat{t})$  are background solutions,  $\partial_i N^{Ti} = 0$  and

$$(e^h)_{ij} = \delta_{ij} + h_{ij} + \frac{1}{2} h_{ik} h_{kj} + \frac{1}{6} h_{ik} h_{kl} h_{lj} + \dots , \quad h_{ii} = 0 , \quad \partial_i h_{ij} = 0 .$$

Throughout this paper, we denote the background lapse function by  $N$  instead of  $N_0$ . The residual gauge freedom is fixed by setting  $Y = 0$  and  $W_i^T = 0$ . Variables  $\alpha$ ,  $\beta$  and  $N_i^T$  enter the action without temporal derivatives; the dynamical degrees of freedom are  $\zeta$  and transverse traceless  $h_{ij}$ , i.e., scalar and tensor perturbations. Upon integrating out variables  $\alpha$  and  $\beta$ , one obtains the quadratic actions for scalar and tensor perturbations [44]

$$\mathcal{S}_{\zeta\zeta}^{(2)} = \int d\hat{t} d^3x N a^3 \left[ \frac{\mathcal{G}_S}{N^2} \left( \frac{\partial \zeta}{\partial \hat{t}} \right)^2 - \frac{\mathcal{F}_S}{a^2} \left( \vec{\nabla} \zeta \right)^2 \right] , \quad (14a)$$

$$\mathcal{S}_{hh}^{(2)} = \int d\hat{t} d^3x \frac{N a^3}{8} \left[ \frac{\mathcal{G}_T}{N^2} \left( \frac{\partial h_{ij}}{\partial \hat{t}} \right)^2 - \frac{\mathcal{F}_T}{a^2} h_{ij,k} h_{ij,k} \right] . \quad (14b)$$

Explicit expressions for the coefficients  $\mathcal{G}_S$ ,  $\mathcal{F}_S$ ,  $\mathcal{G}_T$ , and  $\mathcal{F}_T$  in general models of the type (8) as well as equations for background are collected in Appendix A.

## 2.2 Power-law contraction

To build a bouncing model with the early-time behavior (3), we choose the following form [35] of the Lagrangian functions in (8) at early times,  $t \rightarrow -\infty$ :

$$A_2(\hat{t}, N) = \hat{g}(-\hat{t})^{-2\mu-2} \cdot a_2(N) , \quad (15a)$$

$$A_3(\hat{t}, N) = \hat{g}(-\hat{t})^{-2\mu-1} \cdot a_3(N) , \quad (15b)$$

$$A_4 = A_4(\hat{t}) = -B_4(\hat{t}) = -\frac{\hat{g}}{2}(-\hat{t})^{-2\mu} , \quad (15c)$$

where  $\hat{g}$  is some positive constant. Then the equations for background, eqs. (64), take the following form

$$\begin{aligned} \frac{(N a_2)_N}{(-\hat{t})^2} + \frac{3N a_{3N} H}{(-\hat{t})} + 3H^2 &= 0 , \\ \frac{a_2}{(-\hat{t})^2} + 3H^2 - \frac{1}{N} \left[ \frac{(2\mu+1)a_3}{(-\hat{t})^2} - \frac{4\mu H}{(-\hat{t})} - 2 \frac{dH}{d\hat{t}} + \frac{a_{3N}}{(-\hat{t})} \frac{dN}{d\hat{t}} \right] &= 0 , \end{aligned}$$

where  $H$  is the physical Hubble parameter. We make use of the *Ansatz*

$$N = \text{const} , \quad a = d(-t)^\chi , \quad (17)$$

where  $\chi > 0$  is a constant and  $t = N\hat{t}$  is cosmic time, so that  $H = \chi/t$ , and find the algebraic equations for  $N$  and  $\chi$ :

$$(Na_2)_N - 3\chi a_{3N} + 3\frac{\chi^2}{N^2} = 0 , \quad (18a)$$

$$a_2 - \frac{1}{N}(2\mu + 1)\left(a_3 + 2\frac{\chi}{N}\right) + 3\frac{\chi^2}{N^2} = 0 . \quad (18b)$$

In what follows we assume that these equations have a solution with  $N > 0$  and  $1 > \chi > 0$  (the reason for requiring that  $\chi < 1$  will become clear shortly, see also eq. (4)).

Let us emphasize that the form of the Lagrangian functions (15), as well as the entire discussion in this paper, refer to the early contraction stage only. To obtain the bounce itself, as well as subsequent expansion stage, one has to make use of more sophisticated Lagrangian functions that can be obtained, e.g., by gluing procedure elaborated in Ref. [35]. A lesson from Ref. [35] is that designing stable bouncing models with given early-time asymptotics with “strong gravity in the past” is relatively straightforward. In this paper we do not aim at constructing complete cosmological models and stick to early times when the cosmological perturbations are supposed to be generated.

The coefficients entering the quadratic actions (14) for perturbations are straightforwardly calculated by making use of the general expressions (65), (66). In what follows it is convenient to work in cosmic time  $t = N\hat{t}$  and write the quadratic actions in convenient forms (hereafter dot denotes the derivative with respect to cosmic time  $t$ )

$$\mathcal{S}_{hh} = \int dt d^3x \frac{a^3}{8} \left[ \mathcal{G}_T \dot{h}_{ij}^2 - \frac{\mathcal{F}_T}{a^2} h_{ij,k} h_{ij,k} \right] , \quad (19a)$$

$$\mathcal{S}_{\zeta\zeta} = \int dt d^3x a^3 \left[ \mathcal{G}_S \dot{\zeta}^2 - \frac{\mathcal{F}_S}{a^2} \zeta_{,i} \zeta_{,i} \right] . \quad (19b)$$

Then

$$\mathcal{G}_T = \mathcal{F}_T = \frac{g}{(-t)^{2\mu}} , \quad (20)$$

where

$$g = N^{2\mu} \hat{g} , \quad (21)$$

and

$$\mathcal{G}_S = g \frac{g_S}{2(-t)^{2\mu}} , \quad \mathcal{F}_S = g \frac{f_S}{2(-t)^{2\mu}} , \quad (22)$$

with

$$f_S = \frac{2(2 - 4\mu + N^2 a_{3N})}{2\chi - N^2 a_{3N}}, \quad (23a)$$

$$g_S = 2 \left[ \frac{2(2N^3 a_{2N} + N^4 a_{2NN} - 3\chi(2\chi + N^3 a_{3NN}))}{(N^2 a_{3N} - 2\chi)^2} + 3 \right], \quad (23b)$$

where  $a_{2,3}(N)$  and their derivatives are to be evaluated on the solution to eqs. (18), so that  $g$ ,  $f_S$  and  $g_S$  are independent of time. Note that the propagation of the tensor perturbations is luminal,

$$u_T^2 = \frac{\mathcal{F}_T}{\mathcal{G}_T} = 1,$$

whereas the sound speed in the scalar sector is given by

$$u_S^2 = \frac{\mathcal{F}_S}{\mathcal{G}_S} = \frac{f_S}{g_S},$$

and can be substantially smaller than 1.

To end up this Section, we notice that the conformal transformation

$$g_{\mu\nu} = \frac{M_P^2}{2B_4} g_{\mu\nu}^{(E)},$$

where  $M_P = (8\pi G)^{-1/2}$  is the reduced Planck mass, converts the theory into the Einstein frame. In the Einstein frame, the action is cubic Horndeski, and the scale factor is given by eq. (4). This justifies the discussion in Sec. 1 after eq. (4).

### 2.3 Generating perturbations

As pointed out in Introduction, the quadratic actions for perturbations coincide (modulo the fact that  $u_S^2 \neq 1$ ) with the action for tensor perturbation in power-law expansion setup. So, the cosmological perturbations with nearly flat power spectrum may be generated at early contraction epoch. Let us consider for definiteness scalar perturbation  $\zeta$ . It obeys the linearized equation

$$\ddot{\zeta} + \frac{2\mu - 3\chi}{|t|} \dot{\zeta} + \frac{u_S^2 k^2}{d^2 |t|^{2\chi}} \zeta = 0, \quad (24)$$

For  $0 < \chi < 1$ , the mode is effectively subhorizon at early times (in the sense that the effective Hubble time scale  $|t|$  is greater than the period of oscillations  $d \cdot |t|^\chi / (u_S k)$ ), so it is adequately described within the WKB approximation. At later times, the mode is superhorizon; in what follows we consider the case

$$2\mu - 3\chi > 0, \quad (25)$$



in which the superhorizon mode experiences the Hubble friction and freezes out. The horizon exit occurs at time  $t_f(k)$  when

$$\frac{2\mu - 3\chi}{|t_f|} \sim \frac{u_S k}{d|t_f|^\chi},$$

i.e.,

$$|t_f|(k) \sim \left[ \frac{d}{k} \cdot \frac{(2\mu - 3\chi)}{u_S} \right]^{\frac{1}{1-\chi}}. \quad (26)$$

Thus, once the parameters of the theory are chosen in such a way that  $1 > \chi > 0$ ,  $2\mu - 3\chi > 0$ , the perturbations are generated in a straightforward way, *provided that the weak coupling regime occurs all the way down to*  $|t| \sim |t_f|$ . We outline the calculation in Appendix B, and here we give the results for the power spectra:

$$\mathcal{P}_\zeta \equiv \mathcal{A}_\zeta \left( \frac{k}{k_*} \right)^{n_S - 1}, \quad \mathcal{P}_T \equiv \mathcal{A}_T \left( \frac{k}{k_*} \right)^{n_T}, \quad (27)$$

where  $k_*$  is pivot scale, the spectral tilts are

$$n_S - 1 = n_T = 2 \cdot \left( \frac{1 - \mu}{1 - \chi} \right), \quad (28)$$

and the amplitudes are given by

$$\mathcal{A}_\zeta = \frac{1}{g} \cdot \frac{1}{g_S u_S^{2\nu}} \frac{(1 - \chi)^{2\frac{\mu - \chi}{1 - \chi}}}{\pi \sin^2(\nu\pi) \Gamma^2(1 - \nu)} \left( \frac{k_*}{2d} \right)^{2\frac{1 - \mu}{1 - \chi}}, \quad (29a)$$

$$\mathcal{A}_T = \frac{8}{g} \cdot \frac{(1 - \chi)^{2\frac{\mu - \chi}{1 - \chi}}}{\pi \sin^2(\nu\pi) \Gamma^2(1 - \nu)} \left( \frac{k_*}{2d} \right)^{2\frac{1 - \mu}{1 - \chi}}, \quad (29b)$$

where

$$\nu = \frac{1 + 2\mu - 3\chi}{2(1 - \chi)} = \frac{3}{2} + \frac{1 - n_S}{2}. \quad (30)$$

We immediately see from eqs. (29) that the smallness of the scalar and tensor amplitudes is guaranteed by the large value of the overall pre-factor  $\hat{g}$  in eqs. (15), and hence the factor  $g$  given by (21). Also, we see from (29) that the tensor-to-scalar ratio in our model is

$$r = \frac{\mathcal{A}_T}{\mathcal{A}_\zeta} = 8 \frac{f_S^\nu}{g_S^{\nu-1}} = 8 g_S u_S^{2\nu}. \quad (31)$$

This shows that it is not straightforward to have a small value of  $r$ , as required by observations [39, 45, 46], which give

$$r < 0.032.$$

Since  $f_S \leq g_S$  to avoid superluminality, small  $r$  requires that either  $f_S \leq g_S \ll 1$  or  $u_S \ll 1$  or both. It is clear from (23) that obtaining both  $g_S \ll 1$  and  $f_S \ll 1$  requires strong

fine-tuning. On the contrary, eq. (23a) suggests that ensuring that  $f_S \ll 1$  while  $g_S \sim 1$ , and hence  $u_S^2 \ll 1$  may not be so problematic. We give concrete examples in Sec. 3. Thus, the small tensor-to-scalar ratio in our set of models is due to small sound speed of scalar perturbations. This is reminiscent of the situation in k-inflation [47, 48, 49], where the tensor-to-scalar ratio is also suppressed for small  $u_S$ .

We now turn to the scalar and tensor tilts given by eq. (28). First, we note that the two tilts are equal to each other, unlike in most of inflationary models. Second, we point out that approximate flatness of the spectra is ensured in our set of models by choosing  $\mu \approx 1$ , while the slightly red  $\Lambda$ CDM spectrum (6) is found for

$$\mu > 1 .$$

As we discuss below, the small value of  $r$ , especially in the case  $\mu > 1$ , is non-trivial from the viewpoint of the strong coupling problem. Before coming to the strong coupling issue, let us make a point on approximate flatness itself.

## 2.4 Flatness of power spectra and dilatation invariance

Flatness of the power spectra at  $\mu = 1$  is not an accident: the model with  $\mu = 1$  is invariant under scale transformations. Let us see this explicitly.

One immediately observes that for  $\mu = 1$ , the ADM action (8) with the Lagrangian functions given by (15) is invariant under scale transformation

$$\hat{t} = \lambda \hat{t}' , \quad x^i = \lambda x'^i , \quad (N, N_i, \gamma_{ij})(x^i, \hat{t}) = (N', N'_i, \gamma'_{ij})(x'^i, \hat{t}') , \quad (32)$$

with  $\lambda = \text{const}$ . However, in the ADM language this is a somewhat murky point. To clarify it, we move to covariant formalism with the action (7). To this end, we define the field  $\phi$ , without loss of generality, in such a way that

$$-\hat{t} = e^{-\phi} .$$

Then eq. (10) gives

$$N = \frac{e^\phi}{\sqrt{2X}} , \quad (33)$$

and the Lagrangian functions take the following forms

$$\begin{aligned} A_2 &= \hat{g} e^{(2\mu+2)\phi} a_2 \left( \frac{e^\phi}{\sqrt{2X}} \right) , \\ A_3 &= \hat{g} e^{(2\mu+1)\phi} a_3 \left( \frac{e^\phi}{\sqrt{2X}} \right) , \\ B_4 &= -\frac{\hat{g}}{2} e^{2\mu\phi} . \end{aligned}$$

They define the Lagrangian functions  $G_2, G_3, G_4$  in accordance with eqs. (9) and (11).

Now, in covariant formalism we introduce the scale transformation of metric and scalar field,

$$g_{\mu\nu} = \lambda^2 g'_{\mu\nu} , \quad \phi = \phi' - \ln \lambda , \quad (35)$$

so that  $X = \lambda^{-2} X'$ . The combination in the right hand side of eq. (33) is invariant under this transformation. The meaning of this property is that  $N' = \frac{e^{\phi'}}{\sqrt{2X'}}$  (which is actually equal to  $N$ ) is the lapse function in coordinates  $x'^{\mu}$  introduced in (32). With this understanding, it is fairly straightforward to check that the action (7) with  $\mu = 1$  is invariant under scale transformation (35). This is clear from the fact that under scale transformation one has

$$A_2(\phi, X) = \lambda^{-2\mu-2} A_2(\phi', X') , \quad A_3(\phi, X) = \lambda^{-2\mu-1} A_3(\phi', X') , \quad B_4(\phi) = \lambda^{-2\mu} B_4(\phi') ,$$

and  $\square\phi = \lambda^{-2}\square'\phi'$ ,  $R = \lambda^{-2}R'$ . A subtlety here concerns the function  $F$ . Its derivative  $F_X$  transforms as  $F_X = \lambda^{2-2\mu} F'_{X'}$ , as it should, so that one would think that

$$F = \int F_X dX = \lambda^{-2\mu} \int F'_{X'} dX' = \lambda^{-2\mu} F' .$$

This is not quite true, though.  $F_X$  defined by eq. (11) may contain a term  $ce^{2\mu\phi}X^{-1}$ , i.e.,  $F$  may contain a term  $ce^{2\mu\phi} \ln X$ . Then, upon scaling transformation, function  $F$ , and hence functions  $G_2$  and  $G_3$  obtain  $\log\text{-}\lambda$  terms,

$$(G_2)_{\log} = -4c\mu X' e^{2\mu\phi'} \cdot \lambda^{-2\mu-2} \ln \lambda^{-2} , \quad (G_3)_{\log} = -c e^{2\mu\phi'} \cdot \lambda^{-2\mu} \ln \lambda^{-2} .$$

However, their contribution to the action (7) vanishes upon integration by parts, in the same way as in eq. (12). Modulo this subtlety, the functions  $G_2, G_3, G_4$  defined by eqs. (9) and (11), have correct scaling at  $\mu = 1$  which ensures the scale invariance of the theory in covariant formulation.

## 2.5 Tension between small $r$ and strong coupling: preliminaries

In this Section, we discuss in general terms the problematic issue with our mechanism of the generation of the cosmological perturbations at Horndeski bounce. It has to do with the dangerous strong coupling, on the one hand, and the small value of  $r$ , on the other — especially for positive  $(\mu - 1)$  as required for the red scalar tilt. Using a concrete example, we will see in Sec. 3 that the problem may be overcome, but in a quite narrow range of parameters. This makes our mechanism particularly interesting and falsifiable.

In this Section we mostly consider for definiteness the case  $\mu > 1$ , as required by the  $\Lambda$ CDM value of the scalar spectral index (6), see eq. (29a). Our formulas, however, are valid also in the Harrison–Zeldovich case  $\mu = 1, n_S = 1$ . We make specific comments on the latter case in appropriate places.

Taken literally, the model with  $\mu > 1$  suffers strong coupling problem in the asymptotic past,  $t \rightarrow -\infty$ . This has been discussed in detail in Ref. [35] (see also Refs. [32, 33, 34]); here we sketch the argument.

The characteristic classical energy scale in the power-law bounce model is the inverse time scale of evolution,

$$E_{class}(t) = |t|^{-1} .$$

Indeed, both background values of physical quantities and parameters governing the perturbations evolve in power-law manner and get order 1 changes in time interval of order  $|t|$  (as an exception, this does not apply to the scale factor  $a(t)$  for  $\chi \ll 1$ , but does apply to the Hubble parameter, since  $|\dot{H}/H| \sim |t|^{-1}$ ). To see whether this classical energy scale is lower than the quantum strong coupling scale, one has to estimate the latter.

Let us consider first the tensor sector of the model. Its quadratic action is given by eq. (19a); importantly, the coefficient  $\mathcal{G}_T = \mathcal{F}_T$  tends to zero as  $t \rightarrow -\infty$ , see (20). The cubic action reads [50]

$$\mathcal{S}_{hhh}^{(3)} = \int dt a^3 d^3x \left[ \frac{\mathcal{F}_T}{4a^2} \left( h_{ik} h_{jl} - \frac{1}{2} h_{ij} h_{kl} \right) h_{ij,kl} \right] . \quad (36)$$

Thus, the quantum strong coupling energy scale  $E_{strong}$  in the tensor sector is determined by the behavior of  $\mathcal{F}_T$ . To estimate this scale at a given moment of time, we note first that we can rescale spatial coordinates at that moment of time to set

$$a = 1 .$$

Now, if the strong coupling scale  $E_{strong}$  is much higher than the energy scale  $|t|^{-1}$  of the classical evolution, the background can be treated as slowly varying, and at a given moment of time it is natural to introduce canonically normalized field  $h_{ij}^{(c)}$  by

$$h_{ij} = \mathcal{G}_T^{-1/2} h_{ij}^{(c)} .$$

Then the cubic interaction term becomes

$$\mathcal{S}_{hhh}^{(3)} = \int dt d^3x \left[ \frac{\mathcal{F}_T}{4\mathcal{G}_T^{3/2}} \left( h_{ik}^{(c)} h_{jl}^{(c)} - \frac{1}{2} h_{ij}^{(c)} h_{kl}^{(c)} \right) \partial_k \partial_l h_{ij}^{(c)} \right] .$$

On dimensional grounds, the quantum strong coupling scale is estimated as

$$E_{strong}^{TTT} \sim \frac{\mathcal{G}_T^{3/2}}{\mathcal{F}_T} = \frac{g^{1/2}}{|t|^\mu} , \quad (37)$$

where we use (20). This scale is indeed higher than the classical energy scale  $H \sim |t|^{-1}$  provided that

$$|t|^{2\mu-2} < g . \quad (38)$$

As pointed out in Refs. [32, 33, 34, 35], this inequality is indeed valid at arbitrarily large  $|t|$  for  $\mu < 1$ , but *it does not hold in the asymptotic past* for  $\mu > 1$ , as required for the red spectral tilt.

Thus, there is potential tension between the red tilt and the validity of the (semi-)classical field theory treatment, i.e., absence of strong coupling. One may take various attitudes towards this potential problem. First, one may pretend to be ignorant about the situation at very early times, and consider only the evolution at the epoch when the theory is weakly coupled, in the sense that  $|t|^{-1} < E_{strong}$ . Second, one may think of a slow change of the exponent  $\mu = \mu(t)$  from  $\mu < 1$  in the asymptotic past to  $\mu > 1$  at later times, when the perturbations are generated. In any case, however, our calculation of the power spectra in Sec. 2.3 and Appendix B is valid *provided that the WKB evolution before the exit from effective horizon occurs in the weak coupling regime*. This means that the freeze-out time (26) must obey the weak coupling condition (38) for any relevant momentum  $k$ .

In fact, the tensor sector is not problematic in this regard. To see this, we recall that the tensor modes exit the effective horizon at

$$t_f^{(T)}(k) \sim \left(\frac{d}{k}\right)^{\frac{1}{1-x}},$$

(see eq. (26) with  $u_S = 1$  for tensor modes). Then the relation (38) with  $t = t_f^{(T)}$  becomes

$$\frac{1}{g} \left(\frac{d}{k}\right)^{2\frac{\mu-1}{1-x}} \ll 1.$$

The left hand side here is of the order of the tensor amplitude  $\mathcal{A}_T$ , eq. (29b), so that the absence of strong coupling at the horizon exit time is guaranteed by the smallness of the tensor amplitude.

The latter property is actually obvious from the Einstein frame viewpoint. For  $\mu > 1$ , the Einstein frame universe experiences the power-law inflation (5). Strong coupling in the asymptotics  $t \rightarrow -\infty$  ( $t_E \rightarrow 0$ ) is interpreted as a mere fact that the inflationary Hubble parameter  $H_E \sim t_E^{-1}$  formally exceeds  $M_P$  at small  $t_E$ . Now, the tensor amplitude is of order  $H_E^2/M_P^2$  at the exit time from the inflationary horizon; small tensor amplitude means the absence of strong coupling at that time,  $H_E \ll M_P$ .

In the case  $\mu = 1$ , the condition of validity of the classical description is time-independent,

$$g \gg 1.$$

Again, this condition is automatically satisfied provided that the tensor amplitude (29b) is small.

The situation is more subtle in the scalar sector, since the scalar sound speed  $u_S$  is small, as required by the small tensor-to-scalar ratio (see eq. (31)). To appreciate this new aspect,

we consider scalar perturbations whose quadratic action is given by (19b), i.e.,

$$\mathcal{S}_{\zeta\zeta} = \int dt d^3x a^3 \mathcal{G}_S \left[ \dot{\zeta}^2 - \frac{u_S^2}{a^2} \zeta_{,i} \zeta_{,i} \right] .$$

Hereafter we assume, in view of the above discussion, that  $g_S$  in eqs. (22), (23b) is of order 1, and the smallness of  $u_S$  is due to small  $f_S$ . Cubic terms in the action for  $\zeta$  are calculated in Refs. [51, 52, 53, 54]. As we discuss in Sec. 2.6.3 and Appendix C, the most relevant terms reduce to just one term (69) in the cubic action (with  $a = 1$ , as before):

$$\mathcal{S}_{\zeta\zeta\zeta}^{(3)} = \int dt d^3x \Lambda_\zeta \partial^2 \zeta (\partial_i \zeta)^2 , \quad (39)$$

with

$$\Lambda_\zeta = \frac{\mathcal{G}_T^3}{4\Theta^2} ,$$

where  $\partial^2 = \partial_i \partial_i$ , and  $\Theta$  is given by (67b). In our model (15), we have

$$\Theta = g \frac{\vartheta}{|t|^{2\mu+1}} , \quad \vartheta = \frac{1}{2} N^2 a_{3N} - \chi , \quad (40)$$

Thus,

$$\Lambda_\zeta = g \frac{\lambda_\zeta}{|t|^{2\mu-2}} ,$$

where<sup>2</sup>

$$\lambda_\zeta = \frac{1}{4\vartheta^2} = O(1) , \quad (41)$$

for all values of  $u_S$  including  $u_S \ll 1$ . To get rid of the sound speed in the quadratic part of the action, we not only set  $a = 1$ , but rescale the spatial coordinates further,  $x^i = u_S y^i$ . Upon introducing canonically normalized field

$$\zeta^{(c)} = (2\mathcal{G}_S)^{1/2} u_S^{3/2} \zeta ,$$

we obtain the quadratic action in canonical form (with effective sound speed equal to 1), whereas the cubic action becomes

$$\mathcal{S}_{\zeta\zeta\zeta}^{(3)} = \int dt d^3y \Lambda_\zeta (2\mathcal{G}_S)^{-3/2} u_S^{-11/2} \partial_y^2 \zeta^{(c)} (\partial_y \zeta^{(c)})^2 . \quad (42)$$

On dimensional grounds, the strong coupling energy scale is determined by

$$(E_{strong}^{\zeta\zeta\zeta})^{-3} \sim \Lambda_\zeta (\mathcal{G}_S)^{-3/2} u_S^{-11/2} .$$

---

<sup>2</sup>In the model of Sec. 3 the property  $\lambda_\zeta = O(1)$  is valid provided that  $\chi$  is not fine tuned to be very close to 1, which is the case we consider.

Collecting all factors, and omitting factors of order 1, we get

$$E_{strong}^{\zeta\zeta\zeta} \sim \frac{1}{|t|} \left( \frac{g^{1/2} u_S^{11/2}}{|t|^{\mu-1}} \right)^{1/3}. \quad (43)$$

The condition of validity of (semi-)classical approximation,  $E_{strong} > |t|^{-1}$ , now reads

$$\left( \frac{g u_S^{11}}{|t|^{2(\mu-1)}} \right)^{1/6} > 1. \quad (44)$$

For small  $u_S$  it is stronger than the condition (38), i.e., eq. (44) is valid at later times (smaller  $|t|$ ) than eq. (38).

Let us see whether the condition (44) can be satisfied at the times when the relevant modes of perturbations exit the effective horizon. The most dangerous are the longest modes, i.e., the smallest  $k = k_{min}$ . To obtain a rough estimate, we take  $k_{min} \approx k_*$  (the momentum dependence is weak in view of small  $|n_S - 1|$ ), and relate the exit time (26) at  $k = k_*$  with the scalar amplitude (29a). We omit factors of order 1 and obtain

$$t_f^{2(\mu-1)} \sim g \mathcal{A}_\zeta u_S^3.$$

In this way we find

$$\left( \frac{g u_S^{11}}{|t_f(k_{min})|^{2(\mu-1)}} \right)^{1/6} \sim \left( \frac{u_S^8}{\mathcal{A}_\zeta} \right)^{1/6} \sim \left( \frac{r^{4/\nu}}{\mathcal{A}_\zeta} \right)^{1/6},$$

where we make use of eq. (31) with  $\nu$  given by (30). So, the validity condition (44) for our weak coupling calculations is roughly

$$\left( \frac{r^{4/\nu}}{\mathcal{A}_\zeta} \right)^{1/6} > 1. \quad (45)$$

We see that there is an interplay between two small numbers,  $r$  and  $\mathcal{A}_\zeta$ . For a crude estimate, we take  $\chi \ll 1$  and  $\mu \approx 1$ , consistent with small  $(1 - n_S)$  as given by (28). Then  $\nu \approx 3/2$ . If we then take, as an example,  $r = 0.02$  and insert  $\mathcal{A}_\zeta \simeq 2 \cdot 10^{-9}$  into the left hand side of eq. (45), we obtain its numerical value approximately equal to 5, suspiciously close to 1. The lesson we learn from this back-of-envelope estimate is twofold. First, one cannot neglect numerical factors “of order 1” here. In particular, one has to be more precise when evaluating the strong coupling scale  $E_{strong}$ : instead of naive dimensional analysis, one has to consider unitarity bounds. We study this point in general terms in Sec. 2.6 and apply the results to a concrete model in Sec. 3. Second, it is clear that one cannot have arbitrarily small tensor-to-scalar ratio  $r$  in our class of models; indeed,  $r \simeq 0.02$  appears to be already on the

edge of the validity of the weakly coupled description that we make use of. We substantiate the latter observation in Sec. 3 within the concrete model.

The above analysis goes through also in the case  $\mu = 1$ ,  $n_S = 1$ . Instead of (44), we obtain the condition for the absence of strong coupling, which is again time-independent,

$$(gu_S^{11})^{1/6} > 1. \quad (46)$$

With  $\nu = 3/2$  this gives

$$\left(\frac{r^{8/3}}{\mathcal{A}_\zeta}\right)^{1/6} > 1,$$

which is similar to (45). We refine this qualitative argument in Sec. 3.

## 2.6 Tree level unitarity and strong coupling energy scale

### 2.6.1 Unitarity relations with different sound speeds

The quantum energy scale of strong coupling is conveniently evaluated by making use of the unitarity bounds on partial wave amplitudes (PWAs) of  $2 \rightarrow 2$  scattering [55, 56, 57, 58]. In our model we have nine  $2 \rightarrow 2$  channels, which we collectively denote by  $\alpha\beta$ , where  $\alpha = (\alpha1, \alpha2)$  and  $\beta = (\beta1, \beta2)$  refer to initial state and final state, respectively:

$$\alpha1, \alpha2 \rightarrow \beta1, \beta2 = \zeta\zeta \rightarrow \zeta\zeta, \quad (47a)$$

$$\zeta h \rightarrow \zeta\zeta, \quad \zeta\zeta \rightarrow \zeta h \quad (47b)$$

$$\zeta h \rightarrow \zeta h \quad (47c)$$

$$\zeta\zeta \rightarrow hh, \quad hh \rightarrow \zeta\zeta \quad (47d)$$

$$\zeta h \rightarrow hh, \quad hh \rightarrow \zeta h \quad (47e)$$

$$hh \rightarrow hh. \quad (47f)$$

An additional complication is that the perturbations  $\zeta$  and  $h$  have different sound speeds.

In this situation a (fairly obvious) generalization of the PWA unitarity relation is [59]

$$\text{Im } a_{\alpha\beta}^{(l)} = \sum_{\gamma} a_{\alpha\gamma}^{(l)} \frac{g_{\gamma}}{u_{\gamma1} u_{\gamma2} (u_{\gamma1} + u_{\gamma2})} a_{\gamma\beta}^{(l)*}, \quad (48)$$

where  $a_{\alpha\beta}^{(l)}$  is PWA with angular momentum  $l$  and initial and final states  $\alpha$  and  $\beta$ , respectively,  $\gamma$  refers to two particles in the intermediate state with sound speeds  $u_{\gamma1}$  and  $u_{\gamma2}$ , and  $g_{\gamma} = 2$  if these intermediate particles are distinguishable and  $g_{\gamma} = 1$  if these particles are identical.<sup>3</sup>

---

<sup>3</sup>Equation (48) is not the most general unitarity relation, but it is valid if the right hand side is saturated by the tree level amplitudes. This is sufficient for our purposes.



We omitted contributions to the right hand side due to multiparticle intermediate states, since they can only strengthen the unitarity bound.

Upon redefining

$$\tilde{a}_{\alpha\beta}^{(l)} = \left( \frac{g_\alpha}{u_{\alpha 1} u_{\alpha 2} (u_{\alpha 1} + u_{\alpha 2})} \right)^{1/2} a_{\alpha\beta}^{(l)} \left( \frac{g_\beta}{u_{\beta 1} u_{\beta 2} (u_{\beta 1} + u_{\beta 2})} \right)^{1/2}, \quad (49)$$

we arrive at familiar form of the unitarity relation which we write in the matrix form for the matrix  $\tilde{a}_{\alpha\beta}^{(l)}$ :

$$\text{Im } \tilde{a}^{(l)} = \tilde{a}^{(l)} \tilde{a}^{(l)\dagger}.$$

The most stringent tree level unitarity bound is obtained for the largest eigenvalue of the tree level matrix  $\tilde{a}^{(l)}$  (which is real and symmetric). This bound reads [60]

$$|\text{maximum eigenvalue of } \tilde{a}^{(l)}| \leq \frac{1}{2}.$$

All these properties are derived in detail in Ref. [59].

### 2.6.2 Dimensional analysis for $u_S \ll 1$ .

The model we consider has the large parameter  $u_S^{-1}$  which governs small tensor-to-scalar ratio. So, as we have seen, the earliest time after which we can trust our setup depends on  $u_S$ . Let us see that the dependence of the rescaled amplitudes  $\tilde{a}_{\alpha\beta}^{(l)}$  on  $u_S$  is the only source of refinement of the naive estimate for the time  $t_{cl}$  of the onset of the classical theory (cf. (38))

$$|t_{cl}|^{2\mu-2} \sim g. \quad (50)$$

We restrict ourselves to the cubic order in perturbations; by experience, higher orders are expected not to give anything new [34, 35]. *Let us ignore the fact that  $u_S \ll 1$  for the time being.* Then the entire Lagrangian defined by the functions (15) is proportional to  $g(-t)^{-2\mu}$ , while the only other ‘‘parameter’’ is  $t$  (we ignore constants of order 1). Note that  $g(-t)^{-2\mu}$  has dimension (mass)<sup>2</sup>. So, on dimensional grounds, before rescaling to canonically normalized fields, the terms in the cubic Lagrangian have the following schematic form

$$\frac{g}{|t|^{2\mu}} \cdot (|t|\partial)^n \cdot \partial^2 \cdot \varphi^3,$$

where  $\varphi$  stands collectively for (dimensionless) scalar and tensor perturbations, and, with slight abuse of notations, we do not distinguish temporal and spatial derivatives at this stage. Going to canonically normalized fields  $\varphi^{(c)} \sim (g^{1/2}/|t|^\mu)\varphi$ , we write the cubic Lagrangian as follows

$$\frac{|t|^\mu}{g^{1/2}} \cdot (|t|\partial)^n \cdot \partial^2 \cdot \varphi^{(c)3}. \quad (51)$$

With this cubic coupling, its contribution to the  $2 \rightarrow 2$  amplitude is, schematically,

$$a^{(l)} \sim \frac{((|t|^\mu/g^{1/2})E^2(E|t|^n))^2}{E^2} \sim \frac{|t|^{2\mu-2}}{g}(E|t|)^{2n+2},$$

where  $E$  is the center-of-mass energy, and  $E^2$  in the denominator comes from the propagator, see Fig. 1. This reiterates that ignoring the fact that  $u_S \ll 1$ , one would obtain the estimate (50) for the time of the onset of the classical theory irrespectively of the channel considered: at that time the amplitude at energy scale  $E \sim E_{class} = |t|^{-1}$  saturates the unitarity bound.

Let us now reintroduce  $u_S \ll 1$ . Importantly, the coefficients in the cubic Lagrangian do not contain inverse powers of  $u_S$ , so, no enhancement by  $u_S^{-1}$  occurs due to the cubic Lagrangian itself. Note that this is not entirely trivial. First, the theory involves non-dynamical variables  $\alpha$ ,  $\beta$ ,  $N_i^T$  entering (13). Their expressions  $\alpha(\zeta, h_{ij})$ ,  $\beta(\zeta, h_{ij})$  and  $N_i^T(\zeta, h_{ij})$ , obtained by solving the constraint equations, may in principle be enhanced by inverse powers of  $u_S$ . As a matter of fact, one can check that this is not the case. Second, one may be tempted to use linearized equations of motion when obtaining the cubic action. This would introduce spurious inverse powers of  $u_S$  when inserting  $\partial_i \partial_i \zeta = u_S^{-2} \ddot{\zeta}$ . The latter subtlety is taken care of by working consistently off-shell, as we do in what follows.

Still, the rescaled amplitudes  $\tilde{a}^{(l)}$  acquire the dependence on  $u_S$ . Schematically, the rescaled amplitudes are now

$$\tilde{a}^{(l)} \sim \frac{|t|^{2\mu-2}}{g}(E|t|)^{2n+2}u_S^{-K},$$

where  $K$  depends on the process. Now the time of the onset of the classical theory is determined by

$$|t_{cl}|^{2\mu-2} \sim gu_S^K.$$

The larger  $K$ , the smaller  $|t_{cl}|$ , the later the system enters the classical theory/weak coupling regime. So, to figure out the actual time  $t_{cl}$  (the latest of the “strong coupling times”), we are going to hunt for processes whose rescaled amplitudes are enhanced by  $u_S^{-K}$  with the largest value of  $K$ .

In the case  $\mu = 1$ , the validity condition for (semi-)classical treatment is  $gu_S^K > 1$ , so, again, the strongest bound on the parameters of a model is obtained for the largest value of  $K$ .

### 2.6.3 Hierarchy of rescaled amplitudes

Let us consider tree-level diagrams of the types shown in Fig. 1.

In our class of models, the amplitudes  $\tilde{a}_{\alpha\beta}^{(l)}$  with one and the same energy  $E$  in the center-of-mass frame  $\mathbf{p}_{\alpha 1} = -\mathbf{p}_{\alpha 2}$  and different particles in the initial, final and intermediate states

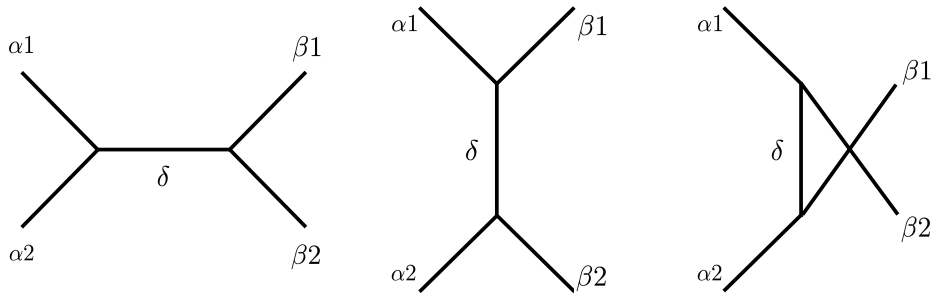


Figure 1: Tree-level diagrams. Particles  $\alpha_1$ ,  $\alpha_2$ ,  $\beta_1$ ,  $\beta_2$  and  $\delta$  can be scalar or tensor.

show hierarchical pattern in terms of the large parameter  $u_S^{-1}$ . This pattern is due to the following properties:

(i) Due solely to rescaling, the rescaled amplitudes (49) are enhanced by a factor  $u_S^{-3/2}$  for two initial (or two final) *scalar* external legs; by a factor  $u_S^{-1/2}$  if initial (or final) legs are  $\zeta h$ ; no enhancement of this sort is associated with two tensor initial (or final) external legs.

(ii) Since the energy and momentum of a *scalar* are related by  $\omega = u_S p$  (we reserve the notation  $E$  for the center-of-mass energy), spatial momentum of an incoming or outgoing scalar may be either of order  $p \sim E/u_S$  or of order  $p \sim E$ . In the former case (only!) every *spatial* derivative in a vertex, that acts on external leg  $\zeta$  gives enhancement  $u_S^{-1}$ . The same observation applies to internal line  $\zeta$  in  $t$ - and  $u$ -channels, if spatial momentum transfer is of order  $E/u_S$ .

(iii) The scalar propagator is given by

$$S(\omega, p) = \frac{1}{\omega^2 - u_S^2 p^2} .$$

For  $\omega = 0$  ( $t$ - and/or  $u$ -channel diagrams with internal line  $\zeta$ ) this gives enhancement  $u_S^{-2}$ , provided that the momentum transfer is  $p \sim E$  (but not  $E/u_S$ ).

To proceed further, we note that the maximum number of *spatial* derivatives in triple- $\zeta$  vertex is 4. In the particular class of Horndeski models (7) with  $G_5 = 0$ , and, furthermore, with  $G_4 = G_4(\phi)$ , there are at most 2 *spatial* derivatives in other vertices. We discuss this point in Appendix C. Another useful observation is that for a given center-of-mass energy  $E$ , incoming (outgoing) momenta are of order  $p \sim E/u_S$  if *both* initial (final) particles are  $\zeta$ , and  $p \sim E$  otherwise.

We now consider various channels and diagrams separately.

**(a).** Purely scalar diagrams, Fig. 2, process (47a). In this case all spatial momenta, including intermediate momentum in  $t$ - and  $u$ -channel diagrams, are of order  $E/u_S$ . Hence, the enhancement mechanisms (i) and (ii) are at work, while the mechanism (iii) is not. The

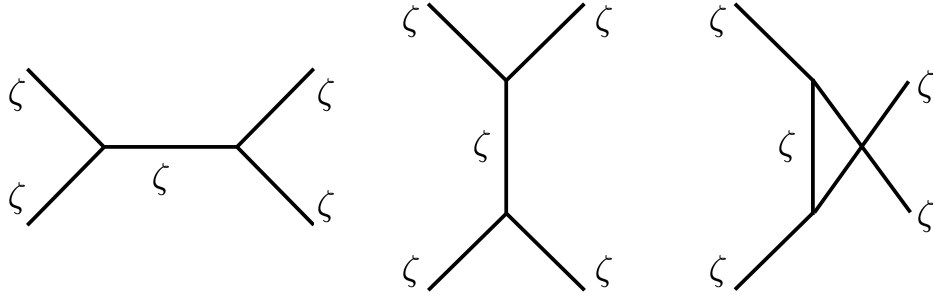


Figure 2: Purely scalar tree-level diagrams: case **(a)**.

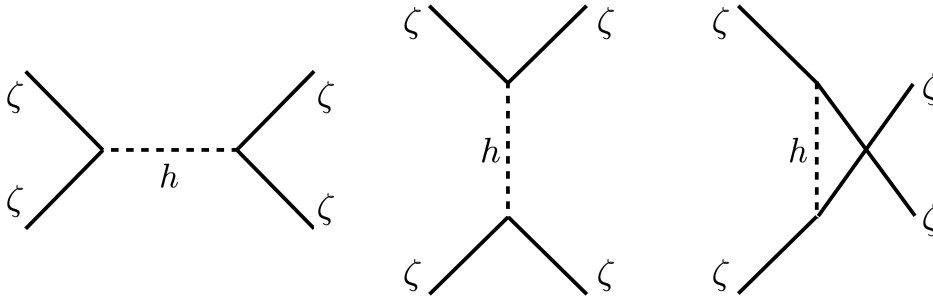


Figure 3: Tree-level diagrams with  $\zeta$ -legs and  $h$ -propagators: case **(b)**.

maximum number of spatial derivatives at each vertex is 4, so the diagrams are of order

$$u_S^{-3/2} \cdot u_S^{-3/2} \cdot 1 \cdot u_S^{-4} \cdot u_S^{-4} = u_S^{-11},$$

(hereafter the first two factors are due to enhancement (i), the third factor due to enhancement (iii) and the last two factors due to enhancement (ii)). This precisely matches the amplitude that one obtains from the cubic action (42).

**(b)**. Strong enhancement would appear to occur also for diagrams with scalar external legs and tensor exchange, Fig. 3. However, as we pointed out, the maximum number of spatial derivatives in each  $\zeta\zeta h$  vertex is 2 (rather than 4). Therefore, the enhancement factor is

$$u_S^{-3/2} \cdot u_S^{-3/2} \cdot 1 \cdot u_S^{-2} \cdot u_S^{-2} = u_S^{-7}. \quad (52)$$

So, tensor exchange gives subdominant contribution.

**(c)**. Process (47b) with  $t$ -channel  $\zeta$ -exchange, Fig. 4, left diagram. The incoming spatial momenta are of order  $E$ , while outgoing ones are of order  $E/u_S$ . So, the spatial momentum transfer is of order  $E/u_S$  and the mechanism (iii) does not work. The enhancement factor is

$$u_S^{-1/2} \cdot u_S^{-3/2} \cdot 1 \cdot u_S^{-2} \cdot u_S^{-4} = u_S^{-8}, \quad (53)$$

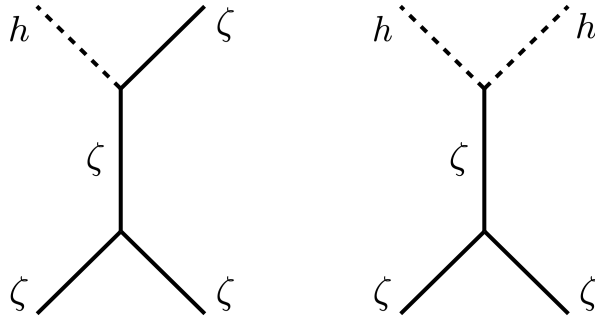


Figure 4: Tree-level  $t$ -channel diagrams: cases **(c)** (left) and **(d)** (right).

so this process is also subdominant.

**(d)**. To illustrate the mechanism (iii), we consider the process (47d) with  $t$ -channel  $\zeta$ -exchange, Fig. 4, right diagram. Spatial momenta of incoming and outgoing particles are of order  $p \sim E$ , the spatial momentum transfer is also of order  $E$ , so the mechanism (ii) does not work. We find the enhancement factor

$$u_S^{-1/2} \cdot u_S^{-1/2} \cdot u_S^{-2} \cdot 1 \cdot 1 = u_S^{-3} , \quad (54)$$

which is again weak.

Other diagrams can be studied in a similar way, and all of them are suppressed as compared to purely scalar process **(a)**. The general argument is straightforward. By replacing one or more external scalar legs in a purely scalar diagram of the case **(a)** by tensor leg(s), one loses at least an enhancement factor  $u_S^{-1}$  from (i) and another factor  $u_S^{-2}$  from (ii). One could in principle gain a factor  $u_S^{-2}$  due to (iii) (we have seen in our example **(c)** that this is actually not the case if one replaces just one scalar leg), but in any case, the overall suppression of a new diagram is at least  $u_S$  as compared to the original, purely scalar one<sup>4</sup>. Replacing the scalar internal line by the tensor line does not improve the situation, and in the particular case **(b)** produces suppressed result.

We conclude that the latest time of the onset of the classical theory  $t_{cl}$  is associated with the scalar sector of the theory. This means, in particular, that the search for the largest eigenvalue of the rescaled PWA matrix  $\tilde{a}$  (Sec. 2.6.1) is unnecessary. The relevant terms in the cubic scalar action are those with four *spatial* derivatives. Modulo numerical factors, the time  $t_{cl}$  is indeed determined from (44),

$$|t_{cl}|^{2\mu-2} \sim g u_S^{11} ,$$

---

<sup>4</sup>In reality the suppression is always even stronger, cf. (52), (53), (54). Moreover, in mixed sectors some couplings in the cubic action are themselves suppressed by positive powers of  $u_S$ , leading to even stronger suppression of the contributions to the amplitudes.

whereas for  $\mu = 1$  the condition is  $gu_S^{11} > 1$ . To refine these estimates, we perform the calculation of the dominant partial wave amplitudes in the scalar sector.

#### 2.6.4 Strong coupling scale from tree-level unitarity

We are now ready to perform the calculation of the strong coupling energy scale, as implied by the tree-level unitarity bound. The (off-shell) cubic action with 4 spatial derivatives in the scalar sector is given by (39). We continue to use the approach of Sec. 2.6.3, set  $a = 1$  as before and work with the field  $\tilde{\zeta} = (2\mathcal{G}_S)^{-1/2}\zeta$ , which has canonical time-derivative term and gradient term with sound speed  $u_S$ . Then the cubic action reads

$$\mathcal{S}_{\zeta\zeta\zeta}^{(3)} = \int dt d^3x \tilde{\Lambda}_\zeta \partial^2 \tilde{\zeta} (\partial \tilde{\zeta})^2,$$

where

$$\tilde{\Lambda}_\zeta = (2\mathcal{G}_S)^{-3/2} \Lambda_\zeta = \frac{\lambda_\zeta |t|^\mu}{g_S^{3/2} g^{1/2}} \cdot |t|^2.$$

It is now straightforward to calculate the  $2 \rightarrow 2$  matrix element  $M(\cos\theta, E)$  as function of scattering angle  $\theta$  and center-of-mass energy  $E$ . We get

$$M = \frac{E^6}{4u_S^8} (1 - \cos^2\theta) \tilde{\Lambda}_\zeta^2,$$

(the origin of the dependence on  $u_S$  is the mechanism (ii) in Sec. 2.6.3). We now write the rescaled PWA amplitude

$$\tilde{a}^{(l)} = \frac{1}{2u_S^3} \cdot \frac{1}{32\pi} \int d(\cos\theta) P_l(\cos\theta) M,$$

where  $P_l$  are Legendre polynomials, the factor  $(2u_S^3)^{-1}$  comes from the redefinition (49) (i.e., it is due to the mechanism (i) in Sec. 2.6.3), and obtain

$$\begin{aligned} \tilde{a}^{(0)} &= \frac{\tilde{\Lambda}_\zeta^2 E^6}{192\pi u_S^{11}}, \\ \tilde{a}^{(2)} &= -\frac{\tilde{\Lambda}_\zeta^2 E^6}{960\pi u_S^{11}}. \end{aligned}$$

The lowest bound on the energy of strong coupling comes from the  $s$ -wave amplitude. It saturates the unitarity bound  $|\tilde{a}^{(0)}| \leq 1/2$  at energy

$$E_{strong}(t) = \left( \frac{96\pi u_S^{11}}{\tilde{\Lambda}^2} \right)^{1/6} = \frac{(96\pi)^{1/6}}{|t|} \left( \frac{g_S^3}{\lambda_\zeta^2} \frac{gu_S^{11}}{|t|^{2\mu-2}} \right)^{1/6}.$$

This refines the estimate (43). Proceeding as in Sec. 2.5, we calculate the ratio of quantum and classical energy scales at the time when the mode  $k_* \approx k_{min}$  exits the effective horizon:

$$\frac{E_{strong}(t_f(k_*))}{E_{class}(t_f(k_*))} \equiv \frac{E_{strong}(k_*)}{E_{class}(k_*)} = E_{strong}(t_f(k_*)) \cdot |t_f(k_*)| = C \cdot \left(\frac{u_S^8}{\mathcal{A}_\zeta}\right)^{1/6}, \quad (56)$$

where

$$C = \frac{96^{1/6} g_S^{1/3}}{|\lambda_\zeta|^{1/3}} \left( \frac{2^{2\frac{\mu-1}{1-\chi}} (1-\chi)^{2\frac{\mu-\chi}{1-\chi}} (2\mu-3\chi)^{2\frac{1-\mu}{1-\chi}}}{\Gamma^2(1-\nu) \sin^2(\nu\pi)} \right)^{1/6}. \quad (57)$$

This is the desired result for general models from the class (15). In the case  $\mu = 1$ ,  $n_S = 1$  (and hence  $\nu = 3/2$ ) we have

$$C = \frac{96^{1/6} g_S^{1/3}}{|\lambda_\zeta|^{1/3}} \left( \frac{(1-\chi)^2}{4\pi} \right)^{1/6}.$$

The result (56) depends in a fairly complicated way, through the parameters  $\chi$ ,  $g_S$  and  $\lambda_\zeta$ , on both the form of the Lagrangian functions ( $a_2(N)$  and  $a_3(N)$  in (15)) and the solution to the equations of motion, eqs. (18). To get an idea of how restrictive the condition for the absence of strong coupling at the horizon exit is, we now turn to concrete examples where all above points are seen explicitly.

### 3 Examples

#### 3.1 $\mu > 1$ , $n_S < 1$ .

In this Section we consider a particular model of the type (15) with the simple forms of the Lagrangian functions:

$$a_2(N) = c_2 + \frac{d_2}{N}, \quad (58a)$$

$$a_3(N) = c_3 + \frac{d_3}{N}, \quad (58b)$$

where  $c_2$ ,  $c_3$ ,  $d_2$ ,  $d_3$ , are dimensionless constants. Making use of eqs. (23), we obtain

$$f_S = -2 \left( \frac{4\mu - 2 + d_3}{2\chi + d_3} \right),$$

$$g_S = \frac{6d_3^2}{(2\chi + d_3)^2}.$$

In accordance with our discussion in Sec. 2.3, one finds that the only way to obtain small tensor-to-scalar ratio (31) is to ensure that  $f_S \ll 1$  and  $g_S \sim 1$ , so that  $u_S^2 = f_S/g_S \ll 1$ .

We begin with the case  $\mu > 1$ , which corresponds to  $n_S < 1$  in accordance with the  $\Lambda$ CDM value (6), and ensure the small value of  $u_S$  by imposing a *fine tuning relation*

$$d_3 = -2 .$$

This choice appears rather remarkable, but we do not know whether it may be a consequence of some symmetry or dynamical principle. Anyway, with this choice, we have

$$f_S = \frac{4(\mu - 1)}{1 - \chi} = 2(1 - n_S) ,$$

$$g_S = \frac{6}{(1 - \chi)^2} ,$$

where we recall eq. (28). Interestingly, small tensor-to-scalar ratio  $r \sim f_S^\nu / g_S^{\nu-1}$  and small scalar tilt  $(1 - n_S)$  are now governed by one and the same small parameter  $(\mu - 1)$ .

Proceeding with  $d_3 = -2$ , we find that equations for the background have relatively simple form. These are algebraic equations:

$$3\chi^2 - 6\chi + c_2 N^2 = 0 ,$$

$$3\chi^2 + 2(2\mu + 1)(1 - \chi) - \kappa N + c_2 N^2 = 0 ,$$

where

$$\kappa = c_3(1 + 2\mu) - d_2 .$$

The relevant solution to these equations is (the second solution does not yield stable bounce)

$$\chi = \frac{3 + 8\rho(\mu - 1)(2\mu + 1) - \sqrt{9 - 12\rho(2\mu + 1)(5 - 2\mu)}}{3 + 16\rho(\mu - 1)^2} ,$$

$$N = \frac{2}{\kappa} [1 + 2\mu - 2(\mu - 1)\chi] ,$$

where

$$\rho = \frac{c_2}{\kappa^2} .$$

While the expression for  $N$  is not of particular physical significance (the only requirement is that  $N > 0$ ), the value of  $\chi$  is an important characteristic of the solution. Note that while  $N$  depends on  $c_2$  and  $\kappa$  separately, the parameter  $\chi$  depends (for given  $\mu$ ) on one combination  $\rho$  out of the three Lagrangian parameters remaining after setting  $d_3 = -2$ . We will see in what follows that  $\mu$  and  $\rho$  (or, equivalently,  $\chi$ ) are the only parameters relevant also for the strong coupling issue.

For small and positive  $(\mu - 1)$ , the allowed range of parameters is

$$\kappa > 0 , \quad 0 < \rho \lesssim \frac{2}{27} .$$



These relations ensure that  $N > 0$  and, importantly,  $2\mu - 3\chi > 0$ , see (25).

We are now equipped with the explicit formulas to see what range of the tensor-to-scalar ratio is consistent with our weak coupling calculations. We obtain from (40), (41)

$$\theta = 1 - \chi, \quad (63a)$$

$$\lambda_\zeta = \frac{1}{4(1 - \chi)^2}, \quad (63b)$$

while the parameter  $\nu$  is still given by (30). Besides the dependence on  $\mu$ , these parameters again depend on  $\rho$  only.

We express the parameter  $\mu$  through  $n_S$  and  $\chi$  using (28). Then we are left with the only free parameter  $\chi$  (or, equivalently,  $\rho$ ). Our final formulas are obtained from (31) and (56):

$$r = 48(1 - \chi)^{2(\nu-1)} \left( \frac{1 - n_S}{3} \right)^\nu,$$

$$\frac{E_{strong}(k_*)}{E_{class}(k_*)} = E_{strong}(t_f(k_*) \cdot |t_f(k_*)|) = \tilde{C} \cdot \left( \frac{r^{4/\nu}}{\mathcal{A}_\zeta} \right)^{1/6},$$

where, as before,  $\nu = 2 - n_S/2$  and

$$\tilde{C} = \frac{C}{(8g_S)^{2/3\nu}},$$

where  $C$  is given by (57), so that

$$\tilde{C} = 2^{\frac{12-11n_S}{24-6n_S}} 3^{\frac{4-3n_S}{24-6n_S}} (1 - \chi)^{\frac{12-n_S}{3(4-n_S)}} \left( \frac{(2 - 2\chi)^{1-n_S} \left( 2 + (1 - n_S) - \chi(3 + (1 - n_S)) \right)^{-(1-n_S)}}{\Gamma^2\left(\frac{n_S}{2} - 1\right) \sin^2 \left[ \left(2 - \frac{n_S}{2}\right)\pi \right]} \right)^{1/6}$$

$$\approx \frac{3^{1/18} (1 - \chi)^{11/9}}{2^{5/18} \pi^{1/6}} = 0.7 \cdot (1 - \chi)^{11/9},$$

where we set  $n_S = 1$  in the last two expressions. In Fig. 5 we show  $r$ -ratio and the ratio  $E_{strong}(k_*)/E_{cl}(k_*)$  as functions of  $\chi$  for the  $\Lambda$ CDM central value  $n_S = 0.9649$  suggested by observations. The main message is that the value of  $r$  is bounded from below in our model,  $r > 0.018$  for  $n_S = 0.9649$ , even for very generous unitarity bound  $E_{strong}(k_*)/E_{cl}(k_*) > 1$ . Note that the parameters should obey  $(2\mu - 3\chi) > 0$  which translates to

$$\chi < \frac{3 - n_S}{4 - n_S} \approx \frac{2}{3}.$$

This bound is also shown in Fig. 5.

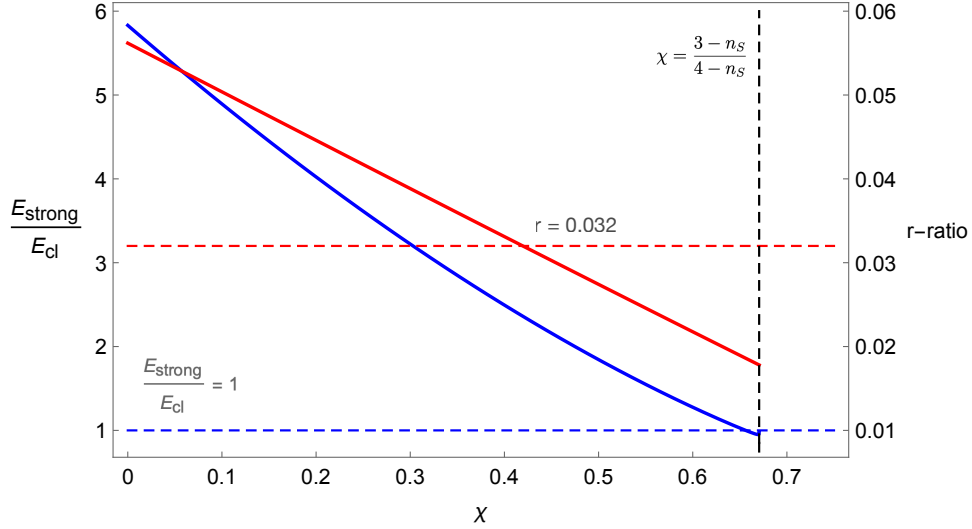


Figure 5: The ratio  $E_{strong}(k_*)/E_{cl}(k_*)$  (blue line) and  $r$ -ratio (red line) as functions of  $\chi$  for the central value  $n_S = 0.9649$ . The allowed range  $r < 0.032$  and the unitarity bound  $E_{strong}(k_*)/E_{cl}(k_*) > 1$  restrict the parameter space to the right lower part.

In Fig. 6 we show what happens if the scalar tilt  $n_S$  is varied within the observationally allowed range. A point to note is that in the entire allowed range, the parameter  $r$  is fairly large,  $r > 0.015$ , while the strong coupling scale is always close to the classical energy scale,  $E_{strong} \lesssim 3E_{cl}$ . We conclude that our simple model is on the verge of being ruled out.

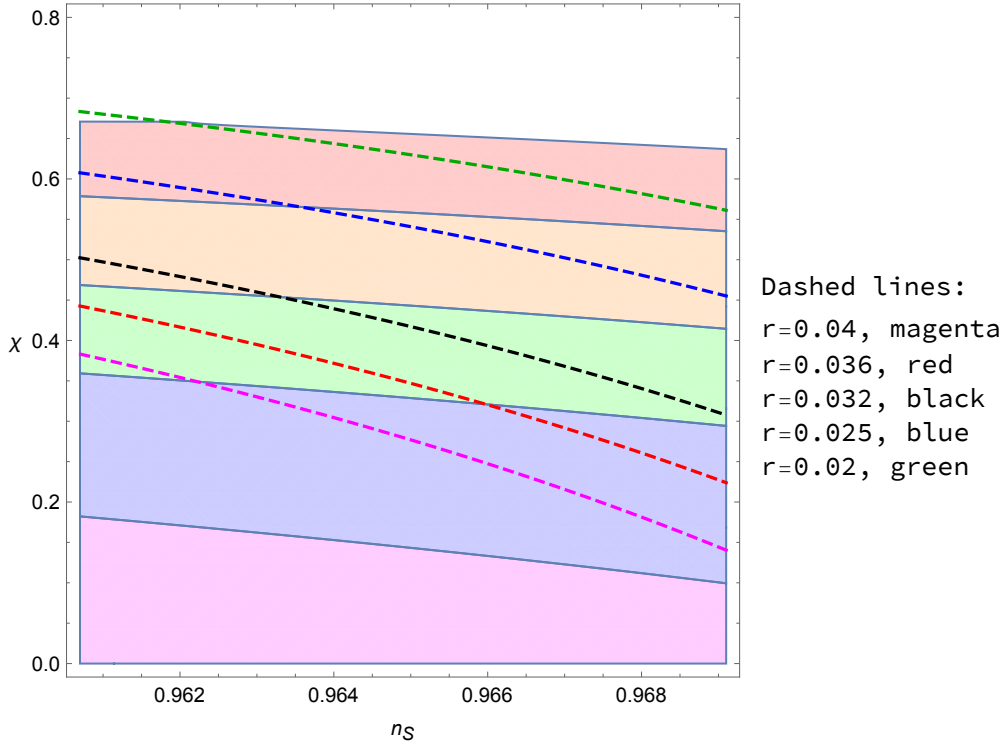


Figure 6: Space of parameters  $n_S$  and  $\chi$ . Colored strips correspond to different ratios of strong coupling scale to classical scale:  $1 < E_{strong}(k_*)/E_{cl}(k_*) < 1.5$  (red),  $1.5 < E_{strong}(k_*)/E_{cl}(k_*) < 2.2$  (orange),  $2.2 < E_{strong}(k_*)/E_{cl}(k_*) < 3$  (green),  $3 < E_{strong}(k_*)/E_{cl}(k_*) < 4.5$  (blue),  $4.5 < E_{strong}(k_*)/E_{cl}(k_*)$  (magenta). Dashed lines show the tensor-to-scalar ratio:  $r = 0.02$  (green),  $r = 0.025$  (blue),  $r = 0.032$  (black),  $r = 0.036$  (red), and  $r = 0.04$  (magenta).

### 3.2 $\mu = 1, n_S = 1$

We now consider the case  $\mu = 1, n_S = 1$  consistent with the early dark energy idea [40, 41]. Our model is still defined by the functions (58), now with  $\mu = 1$ . Unlike in Sec. 3.1, we ensure that  $f_S \ll 1$ , and hence the scalar sound speed is small, by choosing

$$d_3 = -2 + \epsilon, \quad \epsilon \ll 1.$$

Then

$$f_S = \frac{2\epsilon}{2 - 2\chi - \epsilon},$$

$$g_S = \frac{6(2 - \epsilon)^2}{(2 - 2\chi - \epsilon)^2},$$

while  $\theta$  and  $\lambda_\zeta$  are still given by (63). Note that  $\epsilon > 0$ , since we require  $f_S > 0$ .

Background equations of motion are again algebraic, and their solution is

$$\chi = \frac{(2 - \epsilon) \left( 1 + 6\epsilon\rho - \sqrt{1 - 12(1 - \epsilon)\rho} \right)}{2(1 + 3\epsilon^2\rho)},$$

$$N = \frac{3(2 - \epsilon) \left( 2 - \epsilon(1 - \sqrt{1 - 12(1 - \epsilon)\rho}) \right)}{2\kappa(1 + 3\epsilon^2\rho)},$$

with  $\kappa = 3c_3 - d_2$ ,  $\rho = c_2/\kappa^2$ . For given  $\epsilon$ , we can again trade the parameter  $\rho$  for  $\chi$ , hence the two relevant parameters are now  $\chi$  and  $\epsilon$ . Having all formulas above, we are ready to understand what range of the  $r$ -ratio is consistent with the weak coupling regime. We recall (31) and (56), set  $\nu = 3/2$  and find

$$r = \frac{16\epsilon^{3/2}}{[3(2 - 2\chi - \epsilon)]^{1/2}(2 - \epsilon)},$$

$$\frac{E_{strong}}{E_{class}} = \tilde{B} \cdot \left( \frac{r^{8/3}}{\mathcal{A}_\zeta} \right)^{1/6},$$

where the coefficient  $\tilde{B}$  is

$$\tilde{B} = 6^{1/18}(1 - \chi) \left( \frac{[\frac{2-2\chi-\epsilon}{2-\epsilon}]^{4/3}}{4\pi} \right)^{1/6} = 0.7 \cdot (1 - \chi) \left( \frac{2 - 2\chi - \epsilon}{2 - \epsilon} \right)^{2/9}.$$

In Fig. 7 we show  $\frac{E_{strong}}{E_{class}}$  and  $r$  on the plane of the two parameters  $\epsilon$  and  $\chi$ . One observes that in the model with  $\mu = 1$  it is easier to obtain small tensor-to-scalar ratio, still insisting on the generation of the perturbations in the weak coupling regime. Nevertheless, the value of  $r$  cannot be much smaller than 0.01, otherwise one would face with the strong coupling problem.

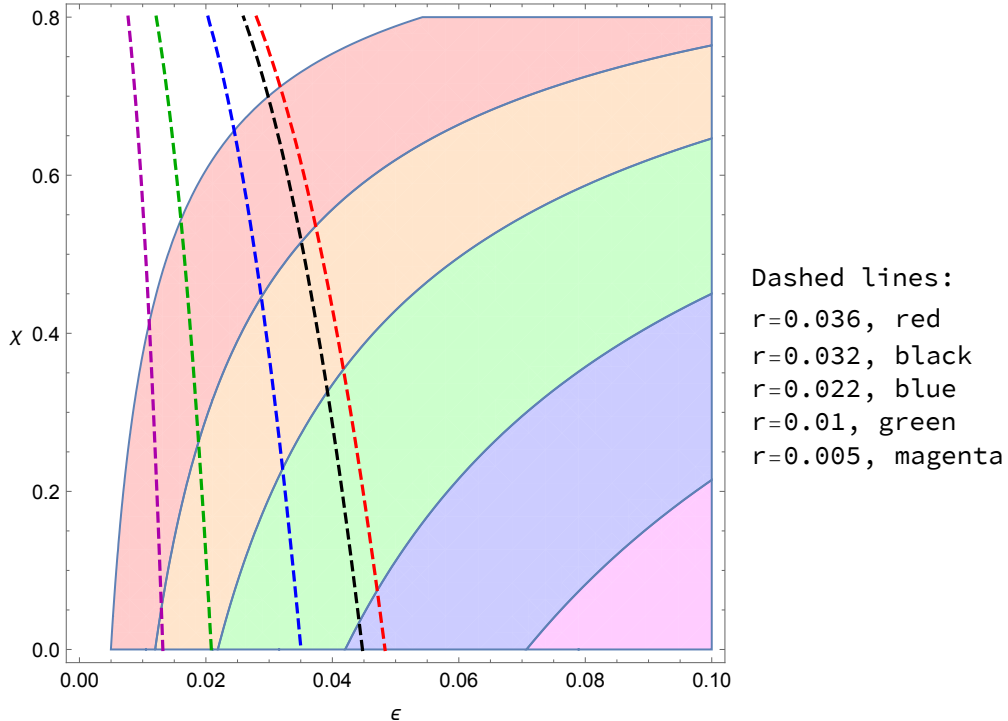


Figure 7: Space of parameters  $\epsilon$  and  $\chi$  in the case  $\mu = 1$ . Colored strips correspond to different ratios of strong coupling scale to classical scale:  $1 < E_{strong}/E_{cl} < 1.8$  (red),  $1.8 < E_{strong}/E_{cl} < 2.7$  (orange),  $2.7 < E_{strong}/E_{cl} < 4.2$  (green),  $4.2 < E_{strong}/E_{cl} < 6$  (blue),  $6 < E_{strong}/E_{cl}$  (magenta). Dashed lines show the tensor-to-scalar ratio:  $r = 0.005$  (magenta),  $r = 0.01$  (green),  $r = 0.022$  (blue),  $r = 0.032$  (black), and  $r = 0.036$  (red).

## 4 Conclusion

In this paper we have studied, in the framework of the Horndeski theory, the contracting cosmological stage which can afterwards pass through bounce to a realistic cosmological expansion, as discussed in detail, e.g., in Ref. [35]. We have found that this stage is capable of producing experimentally consistent scalar power spectrum and small enough tensor-to-scalar ratio  $r$ . Small value of  $(1 - n_S)$  is obtained at the expense of mild fine tuning, while small  $r$  requires small scalar sound speed,  $r \sim u_S^3$ . The latter property is in potential tension with the requirement of weak coupling at the time of the generation of scalar perturbations: small  $u_S$  enhances the scattering amplitudes and modifies the unitarity relation, which is violated at energies dangerously close to the energy scale of the classical evolution. Thus, very small values of  $r$  are strongly disfavored in our class of models. We have illustrated these properties in very concrete examples within the Horndeski theory.

While our motivation originates from the interest in constructing complete, singularity-

free cosmologies, our initial stage of the bounce is conformally equivalent to rapidly expanding Universe, and, indeed, the red scalar tilt is obtained in a model, conformally equivalent<sup>5</sup> to  $G$ -inflation [38]. So, we expect that our observation of the importance of the quantum strong coupling problem may be relevant to the models of  $G$ -inflation, and possibly also  $k$ -inflation. We think this line of thought is worth pursuing in the future.

## Acknowledgements

The authors are grateful to M. Shaposhnikov, A. Starobinsky, A. Westphal, and C. Wetterich for helpful discussions and Yun-Song Piao for useful correspondence. This work has been supported by Russian Science Foundation Grant No. 19-12-00393.

## Appendix A. General expressions in the Horndeski model

Here we give explicit formulas for a theory with action (8). Equations of motion for spatially flat FLRW background read [61]

$$(NA_2)_N + 3NA_{3N}H + 6N^2(N^{-1}A_4)_NH^2 = 0, \quad (64a)$$

$$A_2 - 6A_4H^2 - \frac{1}{N} \frac{d}{dt} (A_3 + 4A_4H) = 0, \quad (64b)$$

where  $H = (Na)^{-1}(da/d\hat{t})$  is the Hubble parameter. The coefficient functions in the quadratic actions for perturbations (14) are given by [44]

$$\mathcal{G}_T = -2A_4, \quad (65a)$$

$$\mathcal{F}_T = 2B_4, \quad (65b)$$

and

$$\mathcal{F}_S = \frac{1}{aN} \frac{d}{dt} \left( \frac{a}{\Theta} \mathcal{G}_T^2 \right) - \mathcal{F}_T, \quad (66a)$$

$$\mathcal{G}_S = \frac{\Sigma}{\Theta^2} \mathcal{G}_T^2 + 3\mathcal{G}_T, \quad (66b)$$

with

$$\Sigma = NA_{2N} + \frac{1}{2}N^2A_{2NN} + \frac{3}{2}N^2A_{3NN}H + 3(2A_4 - 2NA_{4N} + N^2A_{4NN})H^2, \quad (67a)$$

$$\Theta = 2H \left( \frac{NA_{3N}}{4H} - A_4 + NA_{4N} \right). \quad (67b)$$

---

<sup>5</sup>The action for our set of models has fairly simple form in our Jordan frame and is a lot more contrived in the inflationary Einstein frame. For this reason we have performed our analysis entirely in the Jordan frame.

## Appendix B. Power spectra

In this Appendix we present, for completeness, the calculation of the power spectra of perturbations. The quadratic actions for perturbations are given by eqs. (19), where the scale factor is written in eq. (17) and the coefficients are given by eqs. (20), (22).

We give the calculation for the scalar perturbations; tensor perturbations are treated in the same way. We introduce the canonically normalized field  $\psi$  via

$$\zeta = \frac{1}{(2\mathcal{G}_S a^3)^{1/2}} \cdot \psi ,$$

so that the quadratic action is

$$\mathcal{S}_{\psi\psi}^{(2)} = \int d^3x dt \left[ \frac{1}{2} \dot{\psi}^2 + \frac{1}{2} \frac{\ddot{\alpha}}{\alpha} \psi^2 - \frac{u_S^2}{2a^2} (\vec{\nabla} \psi)^2 \right] ,$$

where

$$\alpha = (2\mathcal{G}_S a^3)^{1/2} = \frac{\text{const}}{(-t)^{\frac{2\mu-3\chi}{2}}} .$$

Once the inequality (25) is satisfied, the second term in the integrand is negligible at early times  $t \rightarrow -\infty$ , and the field  $\psi$  can be treated within the WKB approximation. The properly normalized negative-frequency WKB solution is

$$\psi_{WKB} = \frac{1}{(2\pi)^{3/2}} \frac{1}{\sqrt{2\omega}} \cdot e^{-i \int \omega dt} = \frac{1}{(2\pi)^{3/2}} \sqrt{\frac{d}{2u_S k}} (-t)^{\chi/2} \cdot e^{i \frac{u_S}{d} \frac{k}{1-\chi} (-t)^{1-\chi}} ,$$

where

$$\omega = \frac{u_S k}{a} = \frac{u_S \cdot k}{d(-t)^\chi} ,$$

We now solve the complete equation (24) for perturbation  $\zeta$  with the early time asymptotics  $\zeta \rightarrow \zeta_{WKB} = (2\mathcal{G}_S a^3)^{-1/2} \psi_{WKB}$  and obtain

$$\zeta = \mathfrak{C} \cdot (-t)^\delta \cdot H_\nu^{(2)} (\beta(-t)^{1-\chi}) ,$$

where

$$\begin{aligned} \delta &= \frac{1 + 2\mu - 3\chi_1}{2} , \\ \beta &= \frac{u_S k}{d(1-\chi)} , \\ \nu &= \frac{\delta}{\gamma} = \frac{1 + 2\mu - 3\chi}{2(1-\chi)} , \end{aligned}$$

and normalization factor  $\mathfrak{C}$  is found by matching to the WKB solution; modulo an irrelevant time-independent phase, we have

$$\mathfrak{C} = \frac{1}{(gg_S)^{1/2}} \frac{1}{2^{5/2}\pi(1-\chi)^{1/2}} \frac{1}{d^{3/2}} .$$

At late times (formally,  $|t| \rightarrow 0$ ), this solution is time-independent,

$$\zeta = (-i) \frac{\mathfrak{C}}{\sin(\nu\pi)} \frac{(1-\chi)^\nu}{u_S^\nu \Gamma(1-\nu)} \left( \frac{2d}{k} \right)^\nu .$$

It determines the scalar power spectrum via

$$\mathcal{P}_\zeta = 4\pi k^3 \zeta^2 .$$

Collecting all factors, we obtain the result quoted in (27).

Tensor power spectrum is obtained by replacing  $2\mathcal{G}_S \rightarrow \mathcal{G}_T/4$  (i.e.,  $g_S \rightarrow 1/4$ ) and  $u_S \rightarrow u_T = 1$ , and multiplying by 2 due to two tensor polarizations. This gives the result for  $\mathcal{P}_T$  quoted in (27).

## Appendix C. Largest terms in cubic actions.

In this Appendix we collect the expressions for cubic actions that contain the largest number of *spatial* derivatives. As we discuss in the main text, we consistently work off-shell, i.e., do not use equations of motion for dynamical perturbations  $\zeta$ ,  $h_{ij}$  when evaluating the unconstrained cubic action. Neither we employ field redefinitions to get rid of the terms in the cubic action which are proportional to the linearized field equations; we only use the background equations of motion and perform integrations by parts. This is precisely what is done in Refs. [51, 52, 33]. In this approach, no coefficients in the cubic action are enhanced by inverse powers of  $u_S$ . The terms with the largest number of spatial derivatives are readily extracted from Ref. [33]. We stick to the action (7) with  $G_5 = 0$ , or, equivalently, the action (8); furthermore, in our set of models we have  $G_4 = G_4(\phi)$ , or, equivalently,

$$A_4 = -B_4 = -B_4(\hat{t}) ,$$

(no dependence on  $N$ , see eq. (15c)). At a given moment of time we rescale spatial coordinates to set  $a = 1$  as we do in Sec. 2.5 and later in the main text. We work in cosmic time with  $N = 1$ .

We consider various cubic terms in turn.



## C1. Triple- $\zeta$ action.

In the purely scalar sector, the maximum number of spatial derivatives in the cubic action is 4, and the relevant terms, as given in Ref. [33], are

$$\mathcal{S}_{\zeta\zeta\zeta}^{(3)} = \int dt d^3x \left[ \Lambda_7 \dot{\zeta} (\partial^2 \zeta)^2 + \Lambda_8 \zeta (\partial^2 \zeta)^2 + \Lambda_9 \partial^2 \zeta (\partial_i \zeta)^2 + \Lambda_{10} \dot{\zeta} (\partial_i \partial_j \zeta)^2 + \Lambda_{11} \zeta (\partial_i \partial_j \zeta)^2 \right],$$

where, as before,  $\partial^2 = \partial_i \partial_i$  is the spatial Laplacian, and

$$\Lambda_8 = -\Lambda_{11} = -\frac{3\mathcal{G}_T^3}{2\Theta^2}, \quad (68a)$$

$$\Lambda_9 = -\frac{2\mathcal{G}_T^3}{\Theta^2}, \quad (68b)$$

with  $\Lambda_7 = -\Lambda_{10}$ . The function  $\Theta$ , entering (68), is given by (67b), and for the solution in Sec. 2.2, the expression for  $\Theta$  reduces to (40).

One notices that terms with  $\Lambda_7$  and  $\Lambda_{10}$  cancel out upon integration by parts (using  $\Lambda_7 = -\Lambda_{10}$  and neglecting the term of order  $\dot{\Lambda}_{10} \partial_i \partial_j \zeta \partial_i \zeta \partial_j \zeta$ ). Moreover, among the remaining three monomials, only two are independent, modulo integration by parts, since

$$\int d^3x \zeta (\partial_i \partial_j \zeta)^2 = \int d^3x \left[ \zeta (\partial^2 \zeta)^2 + \frac{3}{2} \partial^2 \zeta (\partial_i \zeta)^2 \right].$$

Making use of (68a), one finds that the relevant part of the triple- $\zeta$  action has just one term

$$\mathcal{S}_{\zeta\zeta\zeta}^{(3)} = \int dt d^3x \Lambda_\zeta \partial^2 \zeta (\partial_i \zeta)^2, \quad (69)$$

where

$$\Lambda_\zeta = \Lambda_9 - \frac{3}{2} \Lambda_8 = \frac{\mathcal{G}_T^3}{4\Theta^2}.$$

## C2. $h\zeta\zeta$ , $hh\zeta$ and triple- $h$ actions.

In general Horndeski theory with  $G_5 \neq 0$ , and/or  $G_4 = G_4(\phi, X)$ , the cubic  $h\zeta\zeta$  action has the following general form (see Ref. [54] where explicit expressions are given)

$$\mathcal{S}_{\zeta\zeta h}^{(3)} = \int dt d^3x \left[ c_1 h_{ij} \zeta_{,i} \zeta_{,j} + c_2 \dot{h}_{ij} \zeta_{,i} \zeta_{,j} + c_3 \dot{h}_{ij} \zeta_{,i} \psi_{,j} + c_4 \partial^2 h_{ij} \zeta_{,i} \psi_{,j} + c_5 \partial^2 h_{ij} \zeta_{,i} \zeta_{,j} + c_6 \partial^2 h_{ij} \psi_{,i} \psi_{,j} \right],$$

where

$$\psi = \partial^{-2} \partial_t \zeta.$$

The term with  $c_5$  involves 4 spatial derivatives. However, in the particular case that we consider,  $G_5 = 0$ ,  $G_4 = G_4(\phi)$ , we have

$$c_4 = c_5 = 0 .$$

So, the cubic  $h\zeta\zeta$  action involves 2 spatial derivatives only.

The general structure of the cubic  $\zeta hh$  action is [54]

$$\begin{aligned} \mathcal{S}_{\zeta hh}^{(3)} = \int dt d^3x & \left[ d_1 \zeta \dot{h}_{ij}^2 + \frac{d_2}{a^2} \zeta h_{ij,k} h_{ij,k} + d_3 \psi_{,k} \dot{h}_{ij} h_{ij,k} + d_4 \dot{\zeta} \dot{h}_{ij}^2 \right. \\ & \left. + \frac{d_5}{a^2} \partial^2 \zeta \dot{h}_{ij}^2 + d_6 \psi_{,ij} \dot{h}_{ik} \dot{h}_{jk} + \frac{d_7}{a^2} \zeta_{,ij} \dot{h}_{ik} \dot{h}_{jk} \right] , \end{aligned}$$

and in our case we have

$$d_4 = d_5 = d_6 = d_7 = 0 .$$

The cubic  $\zeta hh$  action also involves at most 2 spatial derivatives.

The cubic action with tensor modes only is given by (36). It involves at most 2 spatial derivatives as well.

## References

- [1] M. Novello and S. E. P. Bergliaffa, Phys. Rept. **463**, 127-213 (2008) doi:10.1016/j.physrep.2008.04.006 [arXiv:0802.1634 [astro-ph]].
- [2] J. L. Lehners, Phys. Rept. **465**, 223-263 (2008) doi:10.1016/j.physrep.2008.06.001 [arXiv:0806.1245 [astro-ph]].
- [3] J. L. Lehners, Class. Quant. Grav. **28**, 204004 (2011) doi:10.1088/0264-9381/28/20/204004 [arXiv:1106.0172 [hep-th]].
- [4] D. Battfeld and P. Peter, Phys. Rept. **571**, 1-66 (2015) doi:10.1016/j.physrep.2014.12.004 [arXiv:1406.2790 [astro-ph.CO]].
- [5] R. Brandenberger and P. Peter, Found. Phys. **47**, no.6, 797-850 (2017) doi:10.1007/s10701-016-0057-0 [arXiv:1603.05834 [hep-th]].
- [6] A. Ijjas and P. J. Steinhardt, Class. Quant. Grav. **35**, no.13, 135004 (2018) doi:10.1088/1361-6382/aac482 [arXiv:1803.01961 [astro-ph.CO]].
- [7] G. W. Horndeski, Int. J. Theor. Phys. **10**, 363-384 (1974) doi:10.1007/BF01807638
- [8] T. Qiu, J. Evslin, Y. F. Cai, M. Li and X. Zhang, JCAP **10**, 036 (2011) doi:10.1088/1475-7516/2011/10/036 [arXiv:1108.0593 [hep-th]].

- [9] D. A. Easson, I. Sawicki and A. Vikman, JCAP **11**, 021 (2011) doi:10.1088/1475-7516/2011/11/021 [arXiv:1109.1047 [hep-th]].
- [10] Y. F. Cai, D. A. Easson and R. Brandenberger, JCAP **08**, 020 (2012) doi:10.1088/1475-7516/2012/08/020 [arXiv:1206.2382 [hep-th]].
- [11] M. Osipov and V. Rubakov, JCAP **11**, 031 (2013) doi:10.1088/1475-7516/2013/11/031 [arXiv:1303.1221 [hep-th]].
- [12] T. Qiu, X. Gao and E. N. Saridakis, Phys. Rev. D **88**, no.4, 043525 (2013) doi:10.1103/PhysRevD.88.043525 [arXiv:1303.2372 [astro-ph.CO]].
- [13] M. Koehn, J. L. Lehnert and B. A. Ovrut, Phys. Rev. D **90**, no.2, 025005 (2014) doi:10.1103/PhysRevD.90.025005 [arXiv:1310.7577 [hep-th]].
- [14] T. Qiu and Y. T. Wang, JHEP **04**, 130 (2015) doi:10.1007/JHEP04(2015)130 [arXiv:1501.03568 [astro-ph.CO]].
- [15] A. Ijjas and P. J. Steinhardt, Phys. Rev. Lett. **117**, no.12, 121304 (2016) doi:10.1103/PhysRevLett.117.121304 [arXiv:1606.08880 [gr-qc]].
- [16] T. Kobayashi, Rept. Prog. Phys. **82**, no.8, 086901 (2019) doi:10.1088/1361-6633/ab2429 [arXiv:1901.07183 [gr-qc]].
- [17] V. E. Volkova, S. A. Mironov and V. A. Rubakov, J. Exp. Theor. Phys. **129**, no.4, 553-565 (2019) doi:10.1134/S1063776119100236 [arXiv:1906.12139 [hep-th]].
- [18] M. Libanov, S. Mironov and V. Rubakov, JCAP **08**, 037 (2016) doi:10.1088/1475-7516/2016/08/037 [arXiv:1605.05992 [hep-th]].
- [19] T. Kobayashi, Phys. Rev. D **94**, no.4, 043511 (2016) doi:10.1103/PhysRevD.94.043511 [arXiv:1606.05831 [hep-th]].
- [20] R. Kolevatov and S. Mironov, Phys. Rev. D **94**, no.12, 123516 (2016) doi:10.1103/PhysRevD.94.123516 [arXiv:1607.04099 [hep-th]].
- [21] S. Akama and T. Kobayashi, Phys. Rev. D **95**, no.6, 064011 (2017) doi:10.1103/PhysRevD.95.064011 [arXiv:1701.02926 [hep-th]].
- [22] Y. Cai and Y. S. Piao, JHEP **09**, 027 (2017) doi:10.1007/JHEP09(2017)027 [arXiv:1705.03401 [gr-qc]].
- [23] R. Kolevatov, S. Mironov, N. Sukhov and V. Volkova, JCAP **08**, 038 (2017) doi:10.1088/1475-7516/2017/08/038 [arXiv:1705.06626 [hep-th]].

- [24] G. Ye and Y. S. Piao, Phys. Rev. D **99**, no.8, 084019 (2019) doi:10.1103/PhysRevD.99.084019 [arXiv:1901.08283 [gr-qc]].
- [25] S. Mironov, V. Rubakov and V. Volkova, Phys. Rev. D **100**, no.8, 083521 (2019) doi:10.1103/PhysRevD.100.083521 [arXiv:1905.06249 [hep-th]].
- [26] A. Ilyas, M. Zhu, Y. Zheng, Y. F. Cai and E. N. Saridakis, JCAP **09**, 002 (2020) doi:10.1088/1475-7516/2020/09/002 [arXiv:2002.08269 [gr-qc]].
- [27] M. Zhu, A. Ilyas, Y. Zheng, Y. F. Cai and E. N. Saridakis, JCAP **11**, no.11, 045 (2021) doi:10.1088/1475-7516/2021/11/045 [arXiv:2108.01339 [gr-qc]].
- [28] M. Zumalacárregui and J. García-Bellido, Phys. Rev. D **89**, 064046 (2014) doi:10.1103/PhysRevD.89.064046 [arXiv:1308.4685 [gr-qc]].
- [29] J. Gleyzes, D. Langlois, F. Piazza and F. Vernizzi, Phys. Rev. Lett. **114**, no.21, 211101 (2015) doi:10.1103/PhysRevLett.114.211101 [arXiv:1404.6495 [hep-th]].
- [30] D. Langlois and K. Noui, JCAP **02**, 034 (2016) doi:10.1088/1475-7516/2016/02/034 [arXiv:1510.06930 [gr-qc]].
- [31] S. Mironov, V. Rubakov and V. Volkova, JHEP **04**, 035 (2021) doi:10.1007/JHEP04(2021)035 [arXiv:2011.14912 [hep-th]].
- [32] Y. A. Ageeva, O. A. Evseev, O. I. Melichev and V. A. Rubakov, EPJ Web Conf. **191**, 07010 (2018) doi:10.1051/epjconf/201819107010 [arXiv:1810.00465 [hep-th]].
- [33] Y. Ageeva, O. Evseev, O. Melichev and V. Rubakov, Phys. Rev. D **102**, no.2, 023519 (2020) doi:10.1103/PhysRevD.102.023519 [arXiv:2003.01202 [hep-th]].
- [34] Y. Ageeva, P. Petrov and V. Rubakov, JHEP **12**, 107 (2020) doi:10.1007/JHEP12(2020)107 [arXiv:2009.05071 [hep-th]].
- [35] Y. Ageeva, P. Petrov and V. Rubakov, Phys. Rev. D **104**, no.6, 063530 (2021) doi:10.1103/PhysRevD.104.063530 [arXiv:2104.13412 [hep-th]].
- [36] D. Nandi, Phys. Lett. B **809**, 135695 (2020) doi:10.1016/j.physletb.2020.135695 [arXiv:2003.02066 [astro-ph.CO]].
- [37] D. Nandi, Universe **7**, no.3, 62 (2021) doi:10.3390/universe7030062 [arXiv:2009.03134 [gr-qc]].
- [38] T. Kobayashi, M. Yamaguchi and J. Yokoyama, Phys. Rev. Lett. **105**, 231302 (2010) doi:10.1103/PhysRevLett.105.231302 [arXiv:1008.0603 [hep-th]].

- [39] N. Aghanim *et al.* [Planck], *Astron. Astrophys.* **641**, A6 (2020) [erratum: *Astron. Astrophys.* **652**, C4 (2021)] doi:10.1051/0004-6361/201833910 [arXiv:1807.06209 [astro-ph.CO]].
- [40] G. Ye, B. Hu and Y. S. Piao, *Phys. Rev. D* **104** (2021) no.6, 063510 doi:10.1103/PhysRevD.104.063510 [arXiv:2103.09729 [astro-ph.CO]].
- [41] J. Q. Jiang and Y. S. Piao, *Phys. Rev. D* **105** (2022) no.10, 103514 doi:10.1103/PhysRevD.105.103514 [arXiv:2202.13379 [astro-ph.CO]].
- [42] J. Gleyzes, D. Langlois, F. Piazza and F. Vernizzi, *JCAP* **08**, 025 (2013) doi:10.1088/1475-7516/2013/08/025 [arXiv:1304.4840 [hep-th]].
- [43] M. Fasiello and S. Renaux-Petel, *JCAP* **10**, 037 (2014) doi:10.1088/1475-7516/2014/10/037 [arXiv:1407.7280 [astro-ph.CO]].
- [44] T. Kobayashi, M. Yamaguchi and J. Yokoyama, *JCAP* **07**, 017 (2015) doi:10.1088/1475-7516/2015/07/017 [arXiv:1504.05710 [hep-th]].
- [45] P. A. R. Ade *et al.* [BICEP and Keck], *Phys. Rev. Lett.* **127**, no.15, 151301 (2021) doi:10.1103/PhysRevLett.127.151301 [arXiv:2110.00483 [astro-ph.CO]].
- [46] M. Tristram, A. J. Banday, K. M. Górski, R. Keskitalo, C. R. Lawrence, K. J. Andersen, R. B. Barreiro, J. Borrill, L. P. L. Colombo and H. K. Eriksen, *et al.* *Phys. Rev. D* **105**, no.8, 083524 (2022) doi:10.1103/PhysRevD.105.083524 [arXiv:2112.07961 [astro-ph.CO]].
- [47] J. Garriga and V. F. Mukhanov, *Phys. Lett. B* **458**, 219-225 (1999) doi:10.1016/S0370-2693(99)00602-4 [arXiv:hep-th/9904176 [hep-th]].
- [48] V. F. Mukhanov and A. Vikman, *JCAP* **02**, 004 (2006) doi:10.1088/1475-7516/2006/02/004 [arXiv:astro-ph/0512066 [astro-ph]].
- [49] D. Langlois, S. Renaux-Petel, D. A. Steer and T. Tanaka, *Phys. Rev. Lett.* **101**, 061301 (2008) doi:10.1103/PhysRevLett.101.061301 [arXiv:0804.3139 [hep-th]].
- [50] X. Gao, T. Kobayashi, M. Yamaguchi and J. Yokoyama, *Phys. Rev. Lett.* **107**, 211301 (2011) doi:10.1103/PhysRevLett.107.211301 [arXiv:1108.3513 [astro-ph.CO]].
- [51] A. De Felice and S. Tsujikawa, *JCAP* **04**, 029 (2011) doi:10.1088/1475-7516/2011/04/029 [arXiv:1103.1172 [astro-ph.CO]].
- [52] X. Gao and D. A. Steer, *JCAP* **12**, 019 (2011) doi:10.1088/1475-7516/2011/12/019 [arXiv:1107.2642 [astro-ph.CO]].

- [53] A. De Felice and S. Tsujikawa, Phys. Rev. D **84**, 083504 (2011) doi:10.1103/PhysRevD.84.083504 [arXiv:1107.3917 [gr-qc]].
- [54] X. Gao, T. Kobayashi, M. Shiraishi, M. Yamaguchi, J. Yokoyama and S. Yokoyama, PTEP **2013**, 053E03 (2013) doi:10.1093/ptep/ptt031 [arXiv:1207.0588 [astro-ph.CO]].
- [55] J. A. Oller, Prog. Part. Nucl. Phys. **110**, 103728 (2020) doi:10.1016/j.pnpnp.2019.103728 [arXiv:1909.00370 [hep-ph]].
- [56] J. A. Oller, *A Brief Introduction to Dispersion Relations. With modern Applications* (Springer Briefs in Physics, Heidelberg, 2019)
- [57] A. Lacour, J. A. Oller and U. G. Meissner, Annals Phys. **326**, 241-306 (2011) doi:10.1016/j.aop.2010.06.012 [arXiv:0906.2349 [nucl-th]].
- [58] D. Gülmez, U. G. Meißner and J. A. Oller, Eur. Phys. J. C **77**, no.7, 460 (2017) doi:10.1140/epjc/s10052-017-5018-z [arXiv:1611.00168 [hep-ph]].
- [59] Y. Ageeva and P. Petrov, “Unitarity relation and unitarity bounds for scalars with different sound speeds,” arXiv:2206.03516 [hep-th].
- [60] C. Grojean, Phys. Usp. **50**, 1-35 (2007) doi:10.1070/PU2007v050n01ABEH006157
- [61] T. Kobayashi, M. Yamaguchi and J. Yokoyama, Prog. Theor. Phys. **126** (2011), 511-529 doi:10.1143/PTP.126.511 [arXiv:1105.5723 [hep-th]].